C2SMART
CONNECTED CITIES WITH SMART TRANSPORTATION
A USDOT University Transportation Center

New York University
Rutgers University
University of Washington
University of Texas at El Paso
The City College of New York

Development of Autonomous Enforcement Approach using Advanced Weigh-In-Motion (A-WIM) System to Minimize Impact of Overweight Trucks on Infrastructure

USDOT Award No. 69A3551747124

September 2021

C2SMART Center is a USDOT Tier 1 University Transportation Center taking on some of today's most pressing urban mobility challenges. Using cities as living laboratories, the center examines transportation problems and field tests novel solutions that draw on unprecedented recent advances in communication and smart technologies. Its research activities are focused on three key areas: Urban Mobility and Connected Citizens; Urban Analytics for Smart Cities; and Resilient, Secure and Smart Transportation Infrastructure.

Some of the key areas C2SMART is focusing on include:

Disruptive Technologies

We are developing innovative solutions that focus on emerging disruptive technologies and their impacts on transportation systems. Our aim is to accelerate technology transfer from the research phase to the real world.

Unconventional Big Data Applications

C2SMART is working to make it possible to safely share data from field tests and non-traditional sensing technologies so that decision-makers can address a wide range of urban mobility problems with the best information available to them.

Impactful Engagement

The center aims to overcome institutional barriers to innovation and hear and meet the needs of city and state stakeholders, including government agencies, policy makers, the private sector, non-profit organizations, and entrepreneurs.

Forward-thinking Training and Development

As an academic institution, we are dedicated to training the workforce of tomorrow to deal with new mobility problems in ways that are not covered in existing transportation curricula.

Led by the New York University Tandon School of Engineering, C2SMART is a consortium of five leading research universities, including Rutgers University, University of Washington, the University of Texas at El Paso, and The City College of New York.

c2smart.engineering.nyu.edu

Feasibility of Autonomous Enforcement using A-WIM System to Reduce Rehabilitation Cost of Infrastructure

Hani Nassif, PE, PhD
Principal Investigator
Rutgers University, New Jersey
ORC-ID: 0000-0002-3441-3589

Kaan Ozbay, PhD
Co-Principal Investigator
New York University, New York
ORC-ID: 0000-0001-7909-6532

Chaekuk Na, PhD
Research Associate
Rutgers University, New Jersey
ORC-ID: 0000-0001-5887-2483

Peng Lou, PhD
Research Associate
Rutgers University, New Jersey
ORC-ID: 0000-0001-7951-1337

Disclaimer

The contents of this report reflect the views of the authors, who are responsible for the facts and the accuracy of the information presented herein. This document is disseminated in the interest of information exchange. The report is funded, partially or entirely, by a grant from the U.S. Department of Transportation's University Transportation Centers Program. However, the U.S. Government assumes no liability for the contents or use thereof.

Acknowledgments

The authors would like to acknowledge the financial support of C2SMART (Connected Cities for Smart Mobility toward Accessible and Resilient Transportation) Tier 1 University Transportation Center at New York University. The authors also would like to thank the New Jersey Turnpike Authority to offer the cost-sharing fund for this study. The authors would like to thank the New York City Department of Transportation (NYCDOT) and New Jersey Department of Transportation (NJDOT) that provided the databases required for the successful completion of this project.

Executive Summary

This study presented the effort to evaluate the damage induced by the overweight (OW) trucks in New York City and to implement the advanced weigh-in-motion (WIM) system for future autonomous OW enforcement practice to one testbed.

First, the bridge and pavement data were aggregated from the NBI database and bridge inspection reports of the NYC bridges and carefully reviewed and analyzed. Accordingly, the team established deterioration models for different types of structures to estimate their socio-economic impact on major highways. The study found that it would be of prime importance to aggregate the bridge inspection and pavement maintenance data from the agency's database for the development of the deterioration models. This would help identify the deterioration modes of different structure types, validate the deterioration models of different structure elements, and accurate life-cycle cost of infrastructure used in the analysis. This study also recommends collecting the bridge element construction and maintenance costs by analyzing the Bid Express bidding service (BIDX system). This is essential to perform a valid and reliable life cycle cost analysis, including labor and material costs, and to quantify the socio-economic impact.

Then, the team worked with NYCDOT to plan and establish a testbed along the triple cantilever of the Brooklyn-Queens Expressway (BQE) corridor to install, collect, and interpret various types of WIM sensors to determine the truck weight spectra effectively. Two testbeds at the north and south portions of the triple cantilever section were considered based on various criteria and constraints aiming to provide more reliable and accurate WIM data. Detailed field surveys, roughness measurement, and recommendations were discussed to select the most appropriate segments for implementation. Two types of WIM sensors (PVDF and Quartz) were installed, and a calibration test was performed to determine the calibration factors and to test the accuracy of the implemented system. It was found that the Quartz sensors provide more reliable and accurate data compared to traditional piezo-type sensors (PVDF). In the end, the quality of WIM data was evaluated based on various quality control and quality assurance (QC/QA) methods. Moreover, the WIM data were analyzed to assess the live loads on the BQE. It was found that more than 10% of total trucks were identified as overweight trucks, and the maximum GVW was found to be more than 200 kips which imposed a significant impact on the NYC highway infrastructure. This confirms that autonomous OW enforcement would be imperative and vital to reducing the extent of the OW trucks.

Table of Contents

List of Figures

List of Tables

1. Introduction

Infrastructure systems, such as roadways and bridges, are major parts of national investment and are critical for the mobility of our society as well as its economic growth and prosperity. Traffic data of infrastructure systems are used to make transportation and freight planning strategies, investigate highway safety, and collect critical traffic input for pavement and bridge designs. In response, federal and local transportation agencies have been collecting traffic data from many existing permanent and fixed weigh-in-motion (WIM) stations across the states. WIM systems are a vital means for weighing the axle or axle group weight and gross vehicle weight (GVW), capturing the axle spacing, and recording the vehicle length, speed, and lane position, while the vehicle is in motion. The collected WIM data will help transportation agencies to understand the actual traffic characteristics, such as truck volume, class configuration, weight distribution, etc., to make their infrastructure safer and more convenient to the taxpayers.

The U.S. Department of Transportation (USDOT) delivered a set of final reports called "Comprehensive Truck Size and Weight Limit Study" in 2016 to address the effect of the oversize and overweight trucks on the safety and risks of infrastructure to comply with the MAP-21 Act (Moving Ahead for Progress in the 21st Century Act). Accordingly, the Transportation Research Board (TRB) established a Truck Size and Weight Limits Research Plan Committee and published a research plan report corresponding to the MAP-21 Act. This report identified five (5) categories and seven (7) core research tracks to address the impacts of federal size and weight regulation changes. The 5 categories include (i) safety, (ii) bridges, (iii) pavements, (iv) enforcement of limits, and (v) shares of freight transported by truck and other modes (TRB Special Report 328, 2018). Accordingly, the report identified 27 research projects under 6 main topics – pavement, bridge, safety, enforcement, mode and vehicle choice and freight market, and cross-cutting topics (evaluation of regulatory options). Among these research projects, some aspects of the first two parts (pavement and bridge) were already studied by the research team in New Jersey and New York City (NYC). The research team developed a procedure to estimate the damage cost of bridges and pavement associated with the overweight trucks for the state of New Jersey (Nassif et al., 2015). A similar approach has been adopted for NYC and reported in Nassif et al. (2018). The team compiled the bridge and pavement maintenance schedule and cost, bridge inspection reports, national bridge inventory, weigh-in-motion (WIM) data, etc., and then developed bridge and pavement deterioration models that account for the weight configuration, bridge and pavement type, design load, etc. to estimate the remaining service life and its service life reduction. Coupled with the life-cycle cost analysis (LCCA) for bridges and pavement, the team was able to quantify the infrastructure damage cost for bridges and pavement induced by the overweight trucks in New Jersey.

The research team has undertaken a study on the enforcement of overweight trucks under the C2SMART project. Traditionally, overweight trucks are enforced by two distinct methods – at the static

weighing station and by traffic enforcement officers using portable weigh scales. However, there is some limitation of these traditional enforcement methods – not all trucks enforced for weight. Especially for the static weighing station, the trucks are guided to enter the static weighing station for the gross vehicle weight (GVW) and axle weight during specific operation hours. The previous study by the research team shows that the overweight trucks are 6.4% of the total truck population per state-wide WIM data; however, the NJDOT report shows that only 0.142% of the total truck population is overweight per state-wide weighing station. The best way to overcome such a gap or the difference in overweight percentage is to monitor the truck weight while the vehicle is on the move.

In this report, the team expands the previous study to develop the deterioration models for the bridges in New York City to estimate the overall infrastructure damage cost induced by the overweight trucks based on the bridge characteristics (National Bridge Inventory (NBI) and bridge inspection reports) coupled with WIM data. This study also includes the continuous effort to establish a testbed to evaluate the advanced WIM (A-WIM) system to use an enforcement tool to identify overweight trucks.

2. Evaluation of the Infrastructure Damage Induced by the Overweight Trucks in New York City

The research team previously developed deterioration models and estimated the damage cost for three (3) bridge types, including prestressed concrete multi-beam bridge, steel multi-beam bridge, and steel girder-floorbeam bridge, and two (2) pavement types including composite and flexible pavements. The team developed the expected bridge condition rating coupled with bridge characteristics from the National Bridge Inventory (NBI) and bridge inspection reports and load history weigh-in-motion (WIM) data. In this project, the team used the same approach to develop deterioration models for the bridges in New York City to estimate the overall infrastructure damage cost induced by the overweight trucks.

2.1 NBI Bridge Database

The National Bridge Inventory (NBI) is a comprehensive database that provides abundant and accurate information about the bridges and tunnels throughout the United States. Every bridge is identified and embodied in the database and its location, features, conditions, etc. In this project, the New York State NBI data from the year 1992 to the year 2016 was used to analyze the bridge's condition rating. To select the target bridge for processing, New York State data were filtered according to the following steps:

- items 4 (Place Code) = 61 (New York County)
- items 5A (Record Type) = 1 (Route carried "on" the structure)
- items 42A (Type of Service); 42A = 1, 4, 5, 6, 7, or 8
    - 1 – Highway
    - 4 – Highway-railroad
    - 5 – Highway-pedestrian
    - 6 – Overpass structure at an interchange or second level of a multilevel interchange
    - 7 – Third level (Interchange)
    - 8 – Fourth level (Interchange))
- item 49 (Structure Length or Bridge Length) >= 6.1meters

- item 112 (NBIS Bridge Length, does structure meet or exceed the minimum length specified to be designated as a bridge for National Bridge Inspection Standards purposes?) = Y (Yes);
- Remove not applicable and blank data
- Remove duplicate data

After filtering, 274 bridges have been selected in the past 25 years. Condition rating of deck, superstructure and substructure were plotted to visualize the tendency.

2.2 NYC Bridge Data Analysis

The mode of bridge deterioration could largely depend on the types of bridges. To precisely develop deterioration models, bridge classification is needed in this project. The bridge was categorized as the following subsection:

- Route Signing Prefix
- Material types
- Structure types

Route Signing Prefix identifies the route signing prefix for the inventory route. It includes the Interstate highway, U.S. numbered highway, state highway, county highway, city street, federal lands road, state lands road, and others. The distribution is shown in Figure 1.

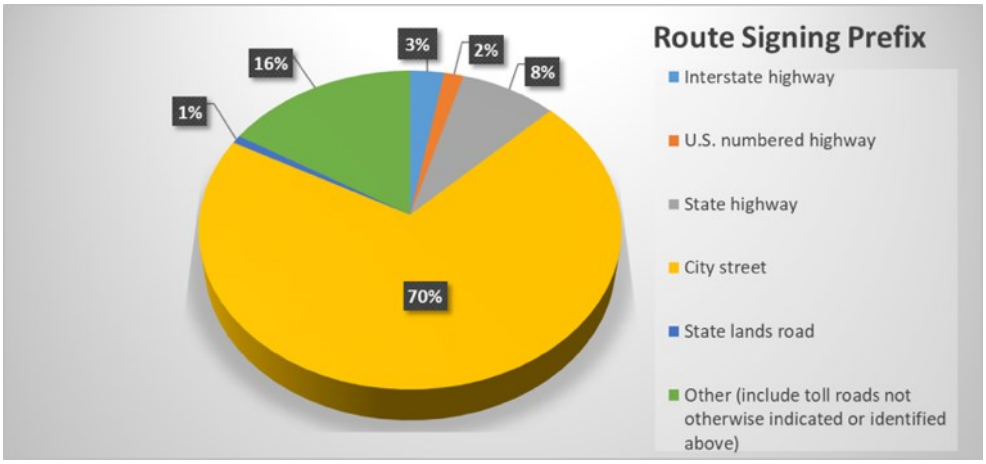

Figure 1: Distribution of Route Signing Prefix in Bridge Inventory

In the NBI database, item 43A classifies the bridge by the material of the superstructure. The material includes concrete, concrete continuous, steel, steel continuous, prestressed concrete, masonry, etc. The distribution is shown in Figure 2. Therefore, the figure shows that the most predominant type of bridge is simply supported steel bridge. More than half of the bridges in New York County are simply supported steel bridges. And the second is the steel continuous bridge.

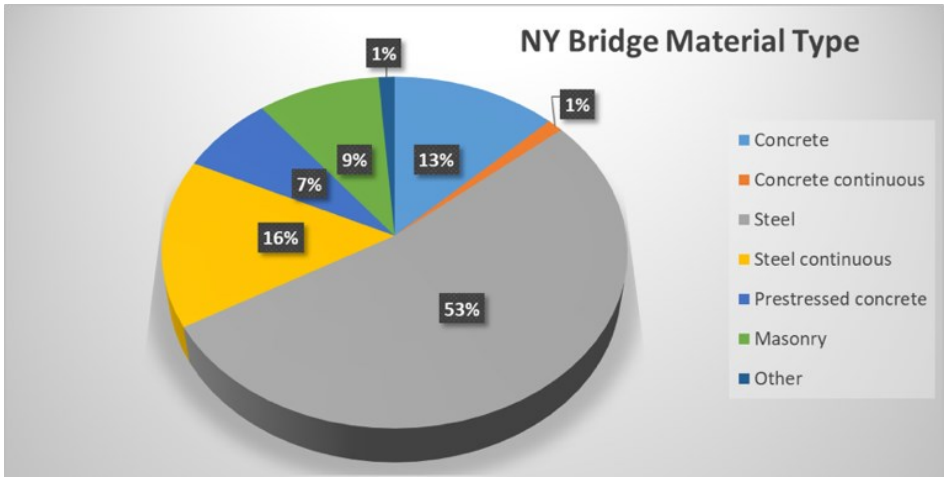

Figure 2: Distribution of Bridge Material Type in Bridge Inventory

Item 43B describes the type of design (structure type) of the bridge. The distribution of each material type was drawn to identify the portion of each structure type in the same material category. Figure 3 to Figure 7 show the structure type distribution in each material type. For the concrete bridge, the culvert structure type (68%) takes the most portion in all types of structure. For steel bridge, girder and floor beam system has the highest percentage of 85, while for steel continuous, most are Stringer/Multi-beam or Girder. For the prestressed bridge, half of the bridges are Stringer/Muti-beam or Girder. And for masonry, all of them are Arch – Deck.

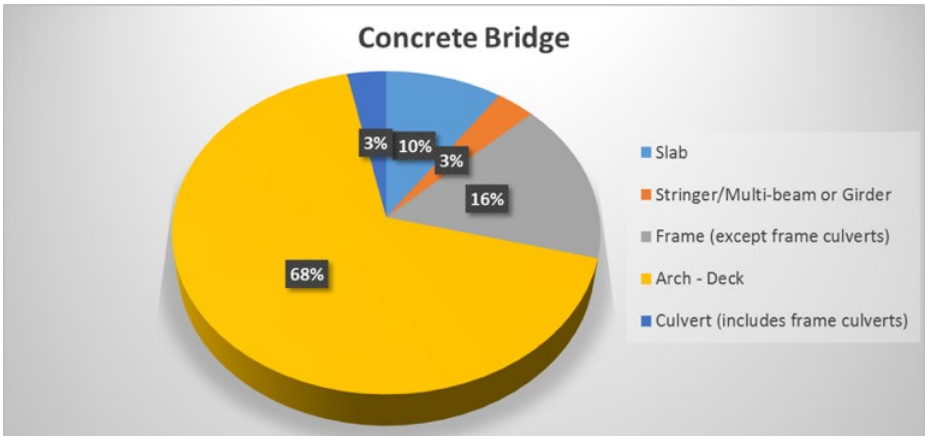

Figure 3: Distribution of Structural Types in Simply Supported Concrete Bridges

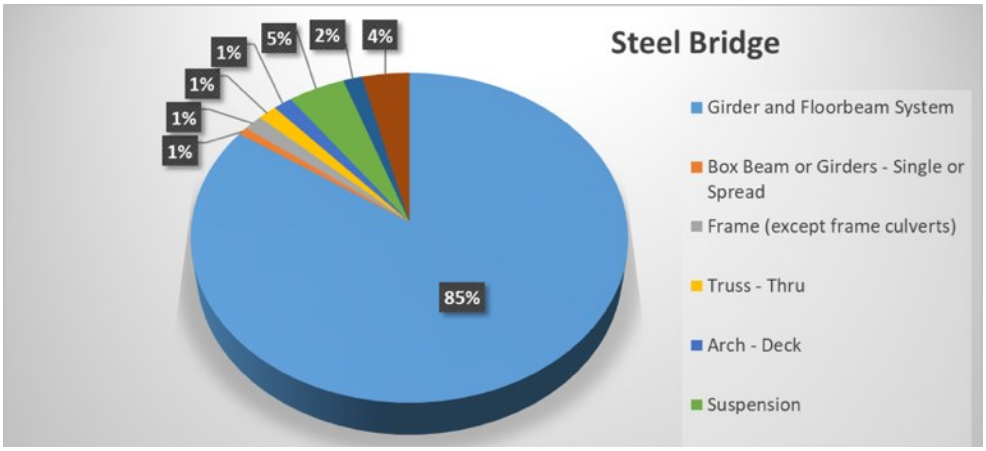

Figure 4: Distribution of Structural Types in Simply Supported Steel Bridges

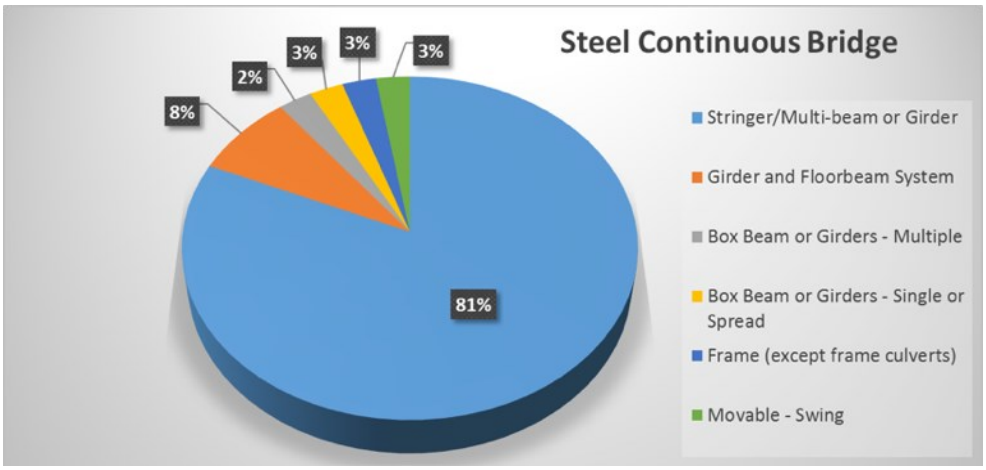

Figure 5: Distribution of Structural Types in Continuous Steel Bridges

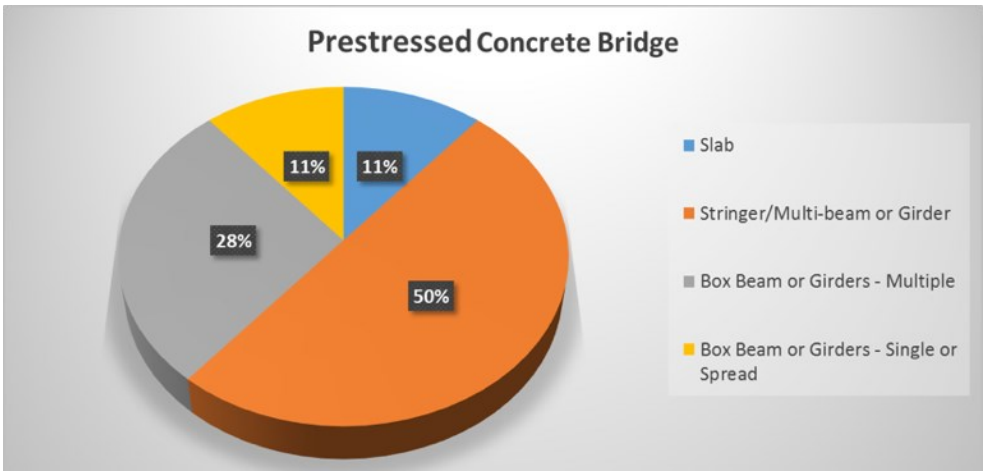

Figure 6: Distribution of Structural Types in Simply Supported Prestressed Concrete Bridge

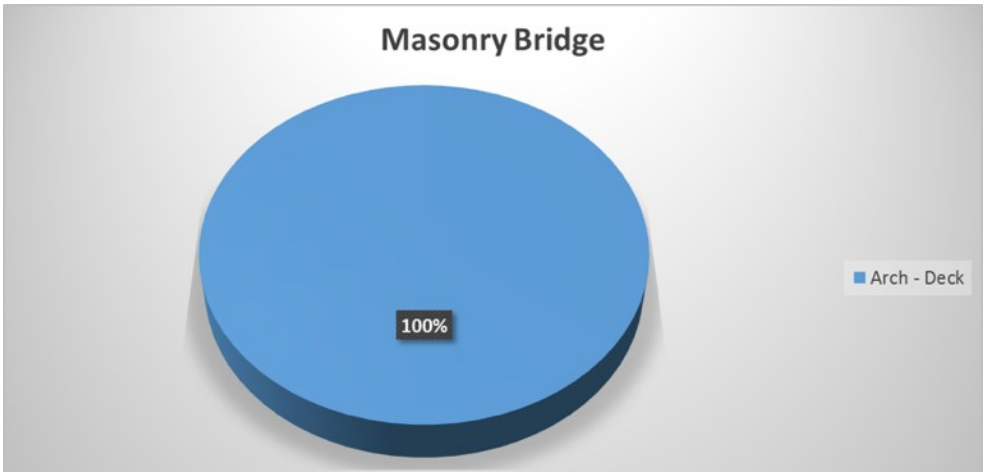

Figure 7: Distribution of Structural Types in Masonry Bridges

2.3 WIM data from NYCDOT

For NYC, the team is currently collaborating with the NYCDOT to establish multiple WIM sites to help the City develop a WIM database to monitor the traffic patterns in NYC. The selection of sites for the installation of WIM systems is based on the traffic pattern, speed restrictions, and the distance from the abutment, but it also depends on the characteristics of the most predominant bridge types in NYC. The team has selected 5 WIM sites shown in Figure 8, and the results of data processing are shown in Table 1. The results show that Site 580 has the highest truck percentage, while Site AHB 041 has the most daily overweight trucks. Site Van Dam, 580, and 280 have a high overweight percentage. The GVW distribution for different sites is shown in Figure 9.

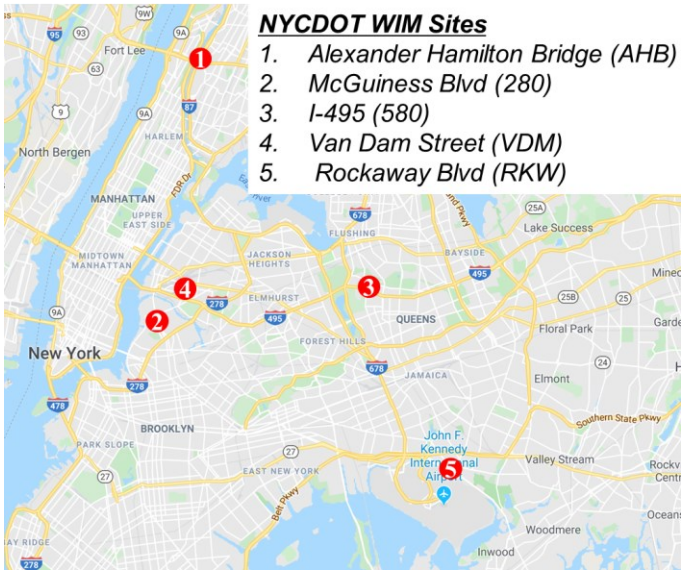

Figure 8: Spatial Locations of the NYCDOT WIM Sites

Site	Year	Days	All Traffic Counts	Trucks Counts	Trucks %	Legal Trucks Counts	OW Trucks Counts	ADTT	Daily Legal	Daily OW	OW%
Van Dam	16	294	10,452,651	532,922	5.10%	417,324	115,598	1,813	1,419	393	21.7%
Van Dam	17	118	4,355,300	190,857	4.38%	152,172	38,685	1,617	1,290	328	20.3%
Rockaway	16	245	9,397,506	473,182	5.04%	396,841	76,341	1,931	1,620	312	16.1%
Rockaway	17	89	3,316,573	160,911	4.85%	137,490	23,421	1,808	1,545	263	14.6%
AHB 041	14	153	10,522,527	1,821,726	17.31%	1,634,840	186,886	11,907	10,685	1,221	10.3%
AHB 041	15	306	23,105,583	4,005,031	17.33%	3,611,045	393,986	13,088	11,801	1,288	9.8%
AHB 041	16	366	27,560,725	4,503,730	16.34%	4,092,103	411,627	12,305	11,181	1,125	9.1%
AHB 041	17	178	12,647,627	1,996,659	15.79%	1,827,674	168,985	11,217	10,268	949	8.5%
580	15	363	2,621,777	1,088,211	41.51%	888,115	200,096	2,998	2,447	551	18.4%
580	16	362	2,229,559	755,455	33.88%	497,110	258,345	2,087	1,373	714	34.2%
580	17	166	1,116,579	683,108	61.18%	485,075	198,033	4,115	2,922	1,193	29.0%
280	15	230	425,703	29,260	6.87%	22,022	7,238	127	96	31	24.7%
280	16	350	662,432	60,346	9.11%	44,693	15,653	172	128	45	25.9%
280	17	165	323,729	30,774	9.51%	23,204	7,570	187	141	46	24.6%

Table 1: WIM Data Processing from Sites in NYC

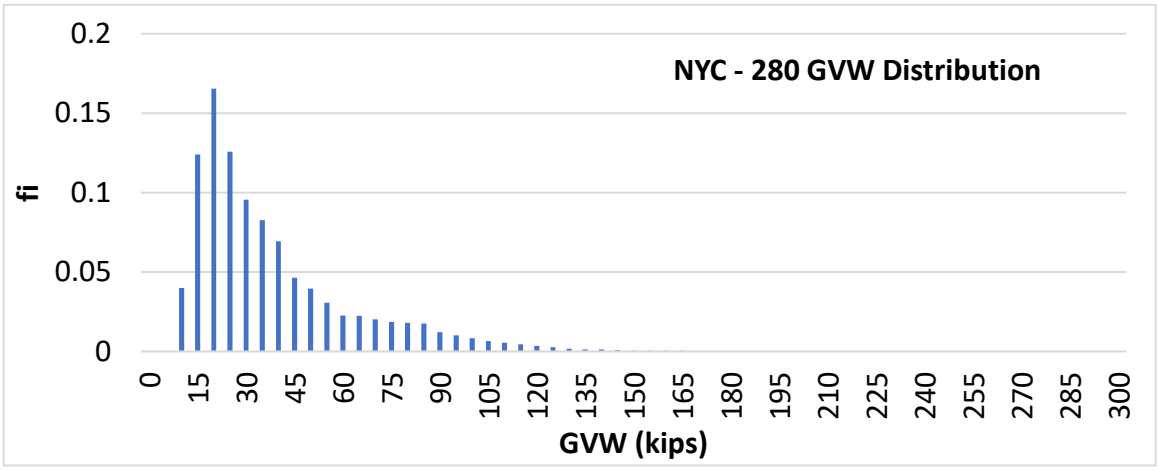

(a) Site 280

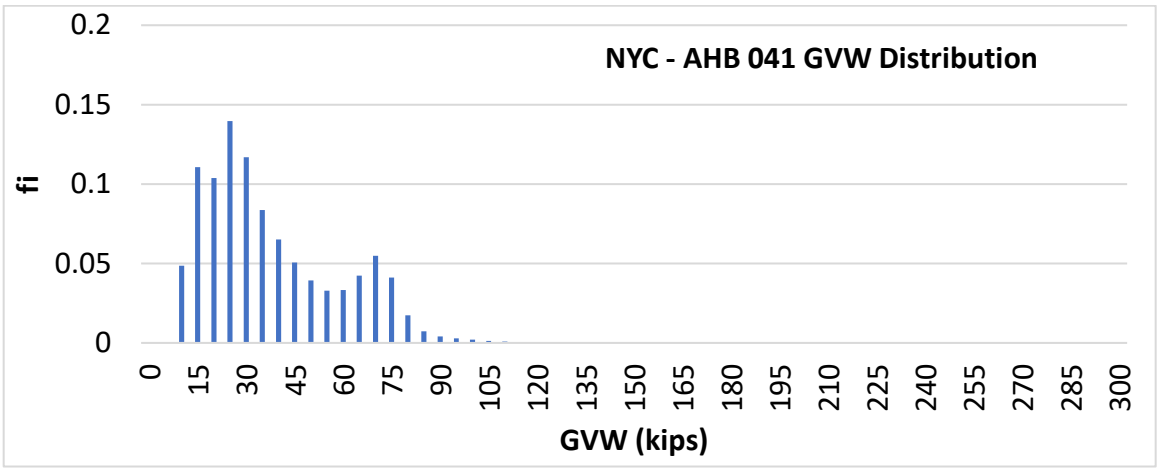

(b) Site AHB 041

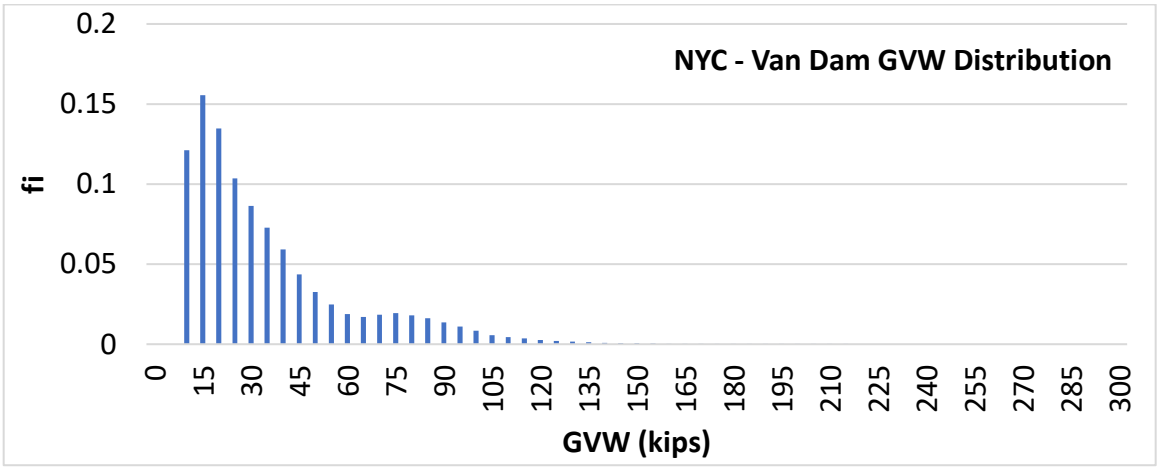

(c) Site Van Dam

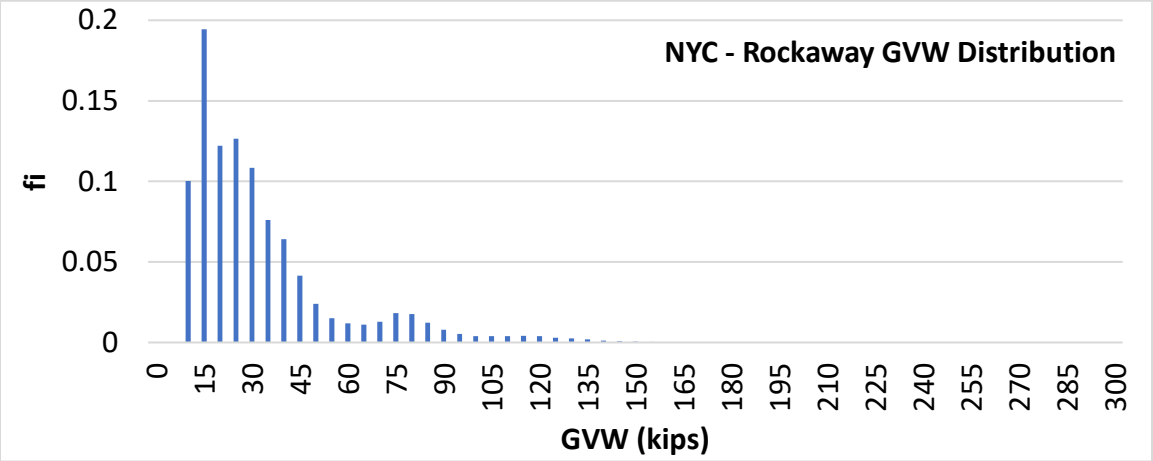

(d) Rockaway

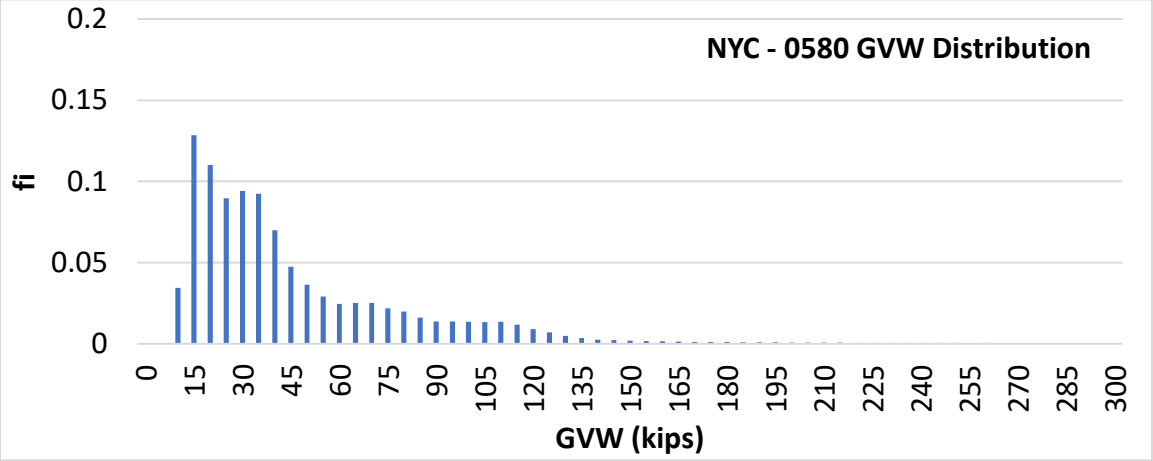

(e) Site 0580

Figure 9: Distribution of GVW from Selected WIM Sites

2.4 Aggregate Bridge Inspection and Pavement Maintenance Data from States' Bridge Database

In this project, the team has collected high-quality bridge inspection data for the selected bridges. The inspection reports are carefully reviewed to identify the typical deteriorations. As an example, the review results are summarized for Washington Bridge, Structure Number 2066919. This bridge has a total of 9 spans, located in the Bronx. The year built is 1888. Important observations are summarized below.

- 10/15/2002
    - Degrade in the pavement: Condition Rating: 4 – 3
- 11/16/2004
    - Degrade in wearing surface: Condition Rating: 4 – 3
- 11/18/2006
    - Upgrade in the pavement for all spans: Condition Rating: 3 - 5
    - Degrade in wearing surface for span 1, 2, 3, and 6: Condition Rating: 5 – 4
- 10/8/2008
    - Degrade in wearing surface for span 1, 2, 3, 6, 7, 8, and 9: Condition Rating: 4 – 3
    - Cracked and delaminated concrete were observed for spans 4, and 5: Condition Rating: 3 – 2
    - Degrade in the joint between span 4, and 5: Condition Rating: 5 – 3
- 11/12/2010
    - Wearing surface conditions for spans 4, and 5 remained unchanged: Condition Rating: 2
    - Joint condition between span 4 and 5 remained unchanged: Condition Rating: 3
- 11/29/2012
    - Upgraded in wearing surface for span 1, 2, 3, 6, 7, 8, and 9: Condition Rating: 3 – 6
    - Upgraded in wearing surface for span 4, and 5: Condition Rating: 2 – 4
    - Degraded in the joint between span 4, and 5: Condition Rating: 3 – 1
- 11/24/2014
    - Degraded in the pavement: Condition Rating: 5 – 3

- Vertical and horizontal fatigue cracks on the primary member with some corrosion on the secondary member (gusset plates) were observed for spans 4, and 5: Condition Rating 5 – 4

- 12/04/2015

  - Pavement condition remained unchanged: Condition Rating: 3

  - Upgraded in the joint between span 4, and 5: Condition Rating: 1 – 3

  - Primary and secondary member conditions for span 4, and 5 remained unchanged: Condition Rating: 4

- 11/19/2016 (Note: CS system begins)

  - Underside of the concrete filled steel grid exhibits scattered areas of paint peeling down to bare steel causing minor surface rust and corrosion to the steel grid/pan, primarily below the sidewalk/roadway interface for span 4, and 5: Condition State: 2. “36, 93, 102, 106”

  - Primary and secondary member condition for spans 4, and 5 remained unchanged: Condition State: 4 (Figure 10). “28, 29, 30, 31, 32, 33, 53, 54, 55, 56, 57, 58”

  - 2 out of 4 missing bolts below the floorbeam at Column #9 Girders G1 located on span 4: Condition State: 3. “38”

  - Missing compression Joint Seal at span 4, and 5: Condition Sate: 4 (Figure 11)

  - Stringer S14 at Floorbeam FB6 located at span 5 exhibits localized moderate corrosion to the lower web with up to 20% section loss due to water leaking thru the intermediate deck joint above. CS - 3 “90”

  - Girder G6 steel arch skewback at Pier 5 located on span 5 exhibits a corrosion hole to the lower web approximately 1" L x 1/2" H surrounded by up to 30% localized section loss: CS - 3. “120”

  - Floorbeam FB6 begin face between Stringer S13 and S14 located at span 5 exhibits a section of the lower web with paint peeling exposing bare metal and moderate corrosion with up to 10% section loss to the lower web. CS – 4. “88”

Figure 10: Vertical and Horizontal Fatigue Cracks on the Left Side of the Web Stiffener

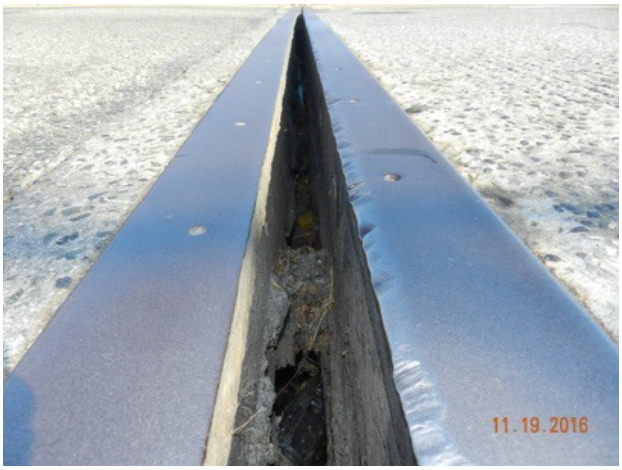

Figure 11: Missing Compression Joint Seal

As a summary, corrosion and section losses are observed mainly at spans 4 and 5 of this structure. Missing compression joint seal could potentially open the path for water to leak thru the intermediate deck joint, therefore lead the steel to corrode. In addition, fatigue cracks are identified at spans 4 and 5. This could be potentially caused by overweight vehicles.

2.5 Collect Cost Data for Bridge and Pavement Construction and Rehabilitation

This section aims to analyze bidding contracts contained in the BIDX system to analyze bridge element construction costs in New Jersey. The BIDX database contains bidding information related to construction contracts issued by the State of New Jersey through the Department of Transportation. According to the itemized data format available in BIDX that reflects how project quantities are computed, it was impossible to extract unit cost per element according to the format of the bridge

management system BrM. However, it was possible to estimate the bounds of the variability of the construction cost for the macro-components, decks, girders, piers, superstructures, substructures, and the entire bridge as a function of the bridge area. These values are summarized in Table 2

	Min [$/sqft]	Mean [$/sqft]	Max [$/sqft]
Deck	118	148	188
Girders	91	134	237
Piers	8	11	15
Superstructure	223	283	411
Substructure	201	304	412
Bridge	469	587	728

Table 2: Bridge Damage Cost for NYC Bridges

3. Implementation of the Advanced Weigh-In-Motion (A-WIM) System and Quartz Sensors

3.1 Brooklyn-Queens Expressway (BQE)

The Brooklyn-Queens Expressway (BQE) was built in 1944 by Robert Moses, connecting the Gowanus Parkway and Robert F. Kennedy Bridge in New York City (Figure 12). Since then, the BQE has been one of the most heavily traveled roadways in New York City and beyond, with average daily traffic (ADT) of 153,000 vehicles. In addition, this corridor is the crucial freight route in New York City, with a peak volume of up to 1,100 trucks per hour (500-600 trucks per direction) during weekday mornings and average daily truck traffic (ADTT) of 25,000 trucks. The triple cantilever section, which splits the BQE on three cantilevers carrying two levels of traffic and Promenade, has been disproportionately impacted by overweight trucks and environmental conditions. Accordingly, the structure has been suffering from extensive deterioration, as shown in Figure 13.

Figure 12: Brooklyn-Queens Bridge Triple Cantilever Picture During Construction (Reference: New York City Parks Photo Archive)

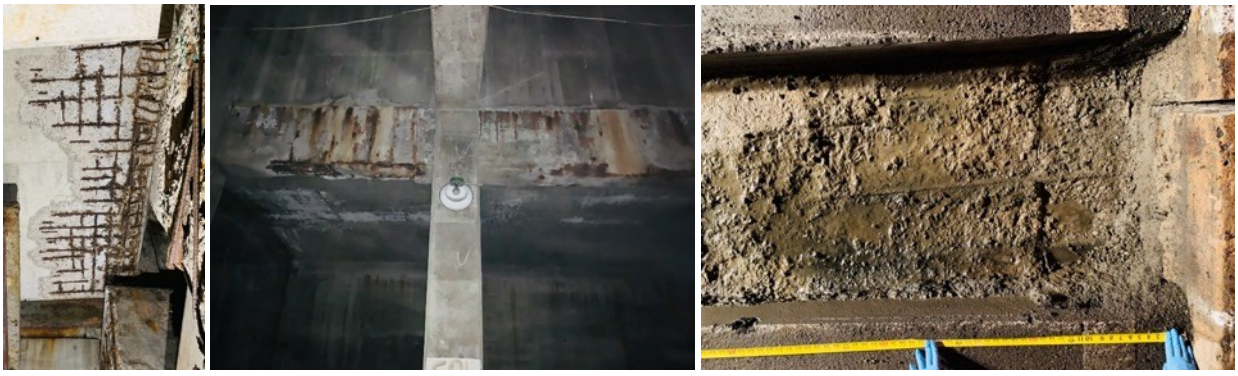

Figure 13: Deteriorated Components of the BQE Triple Cantilever

3.2 Testbeds Selection for A-WIM System

Two WIM sites are proposed to monitor the traffic and truck weight for the BQE. The actual truck traffic can be monitored to determine the loading on the cantilever bridges on BQE in the Brooklyn Height area. Two testbeds were considered, as shown in Figure 14. The first site is in Waterfront District Area, Queens, near Summit Street before Atlantic Avenue. The second site is in Dumbo Area, Queens, between Pearl Street and Adams Street and between Brooklyn Bridge and Manhattan Bridge. These locations were selected to understand the overweight trucks on the triple cantilever. The following criteria were considered to select the most appropriate locations in order to minimize the measurement error.

- Can it identify the OW trucks on the triple cantilever structure?
    - Close to exits – The vehicle will shift lanes.
- Can it be installed on solid ground or structure, not on the bridge?
    - Bridges – The signal-to-noise ratio will be increased due to bridge vibration.
- Can it provide good weighing accuracy?
    - Curved roadway – The vehicle may not stay within a lane.
    - Uphill and downhill – The vehicle will change the speed.

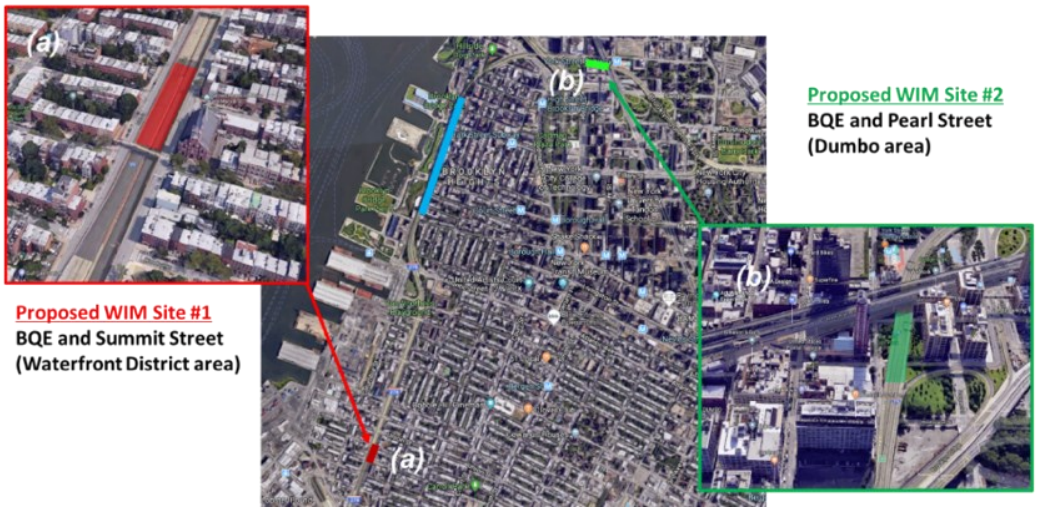

Figure 14: Proposed Testbeds for A-WIM Installation; (a) Site 1 – BQE and Summit Street in Waterfront District Area in Queens, NY, and (b) Site 2 – QBE and Pearl Street in Dumbo Area in Queens, NY

3.3.1 ASTM E1318 Requirement

ASTM E1318 states that an adequate operating environment must be maintained for the WIM system to perform correctly as the system performance, as well as the WIM sensors, may be degraded over time. It emphasizes that the construction or selection of each WIM site is as essential as appropriate routine maintenance and is vital to WIM system performance, testing, and evaluation. Thus, ASTM E1318 defines the roadway requirement for the best performance of the WIM system as below (ASTM E1318).

3.3.1.1 Horizontal Alignment

The horizontal curvature of the roadway lane for 200 ft in advance of and 100 ft beyond the WIM-system sensors shall have a radius not less than 5700 ft measured along the centerline of the lane for all types of WIM systems.

3.3.1.2 Longitudinal Alignment (Profile)

The longitudinal gradient of the road surface for 200 ft in advance of and 100 ft beyond the WIM system sensors shall not exceed 2 % for Type I, Type II, and Type III WIM-system installations and shall not exceed 1 % for Type IV installations.

3.3.1.3 Cross Slope

The cross-slope (lateral slope) of the road surface for 200 ft in advance of and 100 ft beyond the WIM-system sensors shall not exceed 3 % for Type I, Type II, and Type III WIM system installations and shall not exceed 1 % for Type IV installations.

3.3.1.4 Lane Width and Markings

The width of the paved roadway lane for 200 ft in advance of and 100 ft beyond the WIM-system sensors shall be between 12 and 14 ft, inclusive. For Type III, except those with sensors in the main highway lanes and Type IV WIM systems, the edges of the lane throughout this distance shall be marked with solid white longitudinal pavement marking lines 4 to 6 in wide. At least 3 ft of additional clear space for wide loads shall be provided on each side of the WIM-system lane.

3.3.1.5 Surface Smoothness

To allow reliable WIM-system performance within the tolerances, the surface of the paved roadway 200 ft in advance of and 100 ft beyond the WIM-system sensors shall be smooth before sensor installation and maintained in a condition such that a 6-in diameter circular plate 0.125-in. thick cannot be passed beneath a 16-ft long straightedge when the straightedge is positioned and maneuvered.

3.3.2 Review of WIM Site 1 – Summit Street

The Google Earth provides the pavement profiles along the road – inclination and roughness. Although the pavement data is low resolution and may not be accurate, it would give good information to compare the relative pavement condition between segments. The segments between Summit Street and Carroll Street (the north portion of the pedestrian bridge over BQE) were selected based on the research. Figure 15 shows the pavement profile on BQE from Google Earth. Local elevation peaks and relatively high roughness were observed for the Queens Bound (Figure 14(a)). The average slope was 7.3%. This results in the elevation difference being less than 1 ft over 300 ft. Similar roughness and elevation changes were observed for the Staten Island Bound (Figure 14(b)). The average slope was 5.1% (2.2%p less than QB). In both directions, cracks were observed on the pavement.

(a)

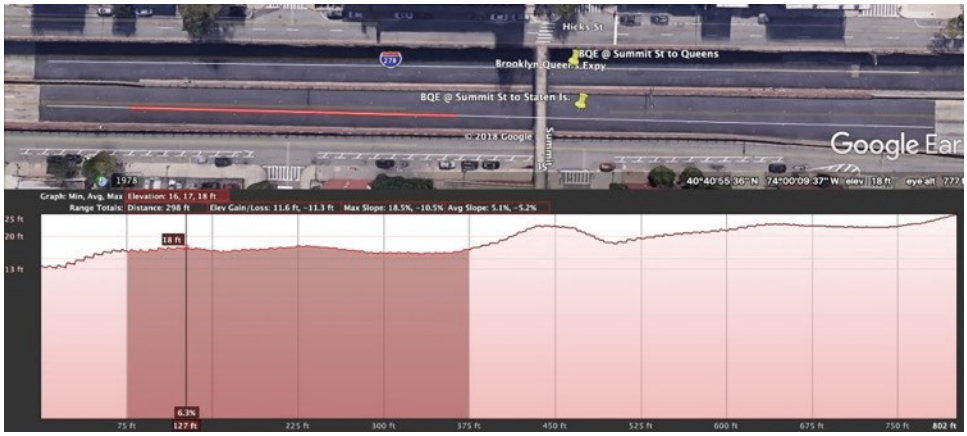

(b)

Figure 15: Pavement Profile at Site 1; (a) Queens Bound (Staten Island to Queens), and (b) Staten Island Bound (Queens to Staten Island) (Reference: Google Earth)

Figure 16 shows some issues found at Site 1. Most large trucks (FHWA Class 6 and up) traveled in the center lane, but the lane width was very narrow. It is estimated less than 10 ft from Google Maps and pictures taken. Also, some rutting was observed on the pavement. Moreover, there were multiple cracks at every 100 ft. which would be shrinkage cracks.

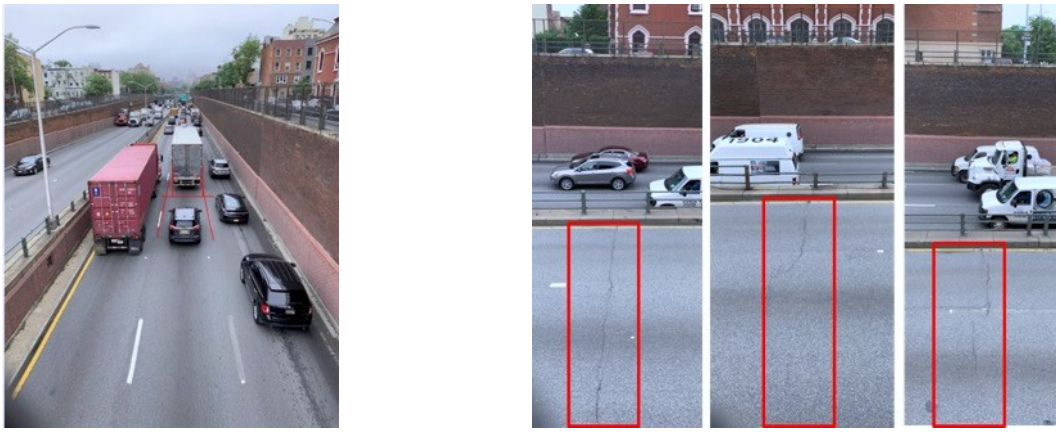

(a) (b)

Figure 16. Field Condition at Site 1; (a) Narrow Lane and (b) Cracks at Every 100 ft

3.3.3 Site 1 Evaluation

The team visited the first WIM site (BQE1) near Summit Street. The team performed a quick survey for the Staten Island Bound (SIB) in the left lane, followed by the QB in the left lane. The team performed an approximate measurement of rutting subsidence in the left lane pavement directly under the wheel path (approx. 1 ft. from each end in the transverse direction) at every 10 ft for 250 ft ~ 300 ft. in the longitudinal direction. For the QB direction, a total length of 300 ft was measured (150 ft. upstream and downstream from the pedestrian bridge). For the SIB direction, a total length of 250 ft was measured (200 ft. upstream and 50 ft. downstream from the pedestrian bridge). The team also measured the approximate height of the pedestrian bridge over the left lane (over the left and right line stripping). The team also measured the lane width and the location of defects such as cracks, drainages, patches, etc.

3.3.3.1 Roadway Configuration

Figure 17 shows the roadway dimension and cross-section of BQE at Summit Street, and Figure 18 shows the height of the pedestrian bridge and lane width for each direction. It was observed that the lane width was approx. 10 ft. except the line stripping. The left lane width for SIB and QB was 122 in. and 121 in., respectively. The roadway width between the median and the retaining wall (curb to curb)

was approx. 38 ft. The total roadway width of SIB and QB was equally distributed to 450 in. The height between the bottom girder of the pedestrian bridge and the pavement varied depending on the lane and location. The height of the pedestrian bridge (between pavement surface and bottom flange of the girder) in the SIB left lane was between 220 in. (over the left line stripping) and 239 in. (over the right line stripping). The height of the pedestrian in the QB left lane was between 259 in. (over the right line stripping) and 278 in. (over the left line stripping). The height difference between the two directions was approx. 68 in.

Based on the field measurement, the height at the center of each lane is estimated in Table 3. The minimum height will be 230 in. (19 ft-2 in) in the center of the QB right lane. The maximum height was 270 in. (22 ft-6 in) in the center of QB's left lane.

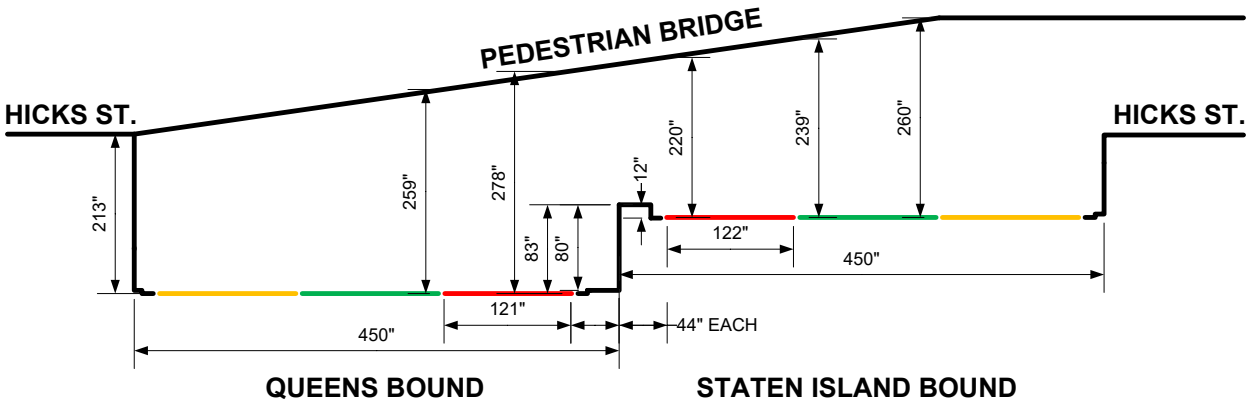

Figure 17: Roadway Dimension and Cross Section of BQE at Summit Street

Direction	Queens Bound			Staten Island Bound		
Lane	Right	Center	Left	Left	Center	Right
Height (ft-in)	230 in. (19 ft-2 in)	250 in. (20 ft-10 in)	270 in. (22 ft-6 in)	230 in. (19 ft-2 in)	250 in. (20 ft-10 in)	260 in. (21 ft-8 in)

Table 3: Estimated Height of Bottom Flange of the Pedestrian Bridge Girder

(a) (b)

Figure 18: Height of Pedestrian and Lane Width of BQE at Summit Street; (a) Staten Island Bound (SIB) and (b) Queens Bound (QB)

3.3.3.2 Pavement Condition

The pavement condition was also reviewed, and several defects were observed. In the SIB direction, 3 transverse cracks, 2 longitudinal cracks, 1 patch, and 1 drainage were observed. The locations of these defects are summarized below.

- Transverse cracks at -23 ft., 67 ft., and 167 ft. (30~36 ft. long)
- Longitudinal cracks on the center lane at 145 ft. and 190 ft. (10~20 ft. long)
- Patch on the center lane at 100 ft. (approx. 12 in. x 6 in.)
- Drainage on the left lane at 10 ft. (approx. 24 in. x 12 in.)

Two defects were observed in the QB direction, and the locations are summarized below.

- Transverse cracks at -20 ft. and 76 ft. (15 ~ 36 ft. long)

3.3.3.3 Pavement Rutting

Figure 19 shows the rutting depths and defects along the left lane for each direction. The team modified the testing procedure per ASTM E1318 to accommodate the constraints of the field. Thus, the team used a 10 ft long and 2 in.x4 in. rectangular wooden straight edge and measured the maximum rutting depth along the roadway.

Based on the field measurement, moderate ruttings were observed. The minimum rutting depth was 2 mm, and the maximum was 20 mm. The maximum rutting was observed at 140 ft. before the pedestrian bridge on QB (see Figure 20). The rutting on the left wheel was 15 mm while that on the right wheel was 20 mm.

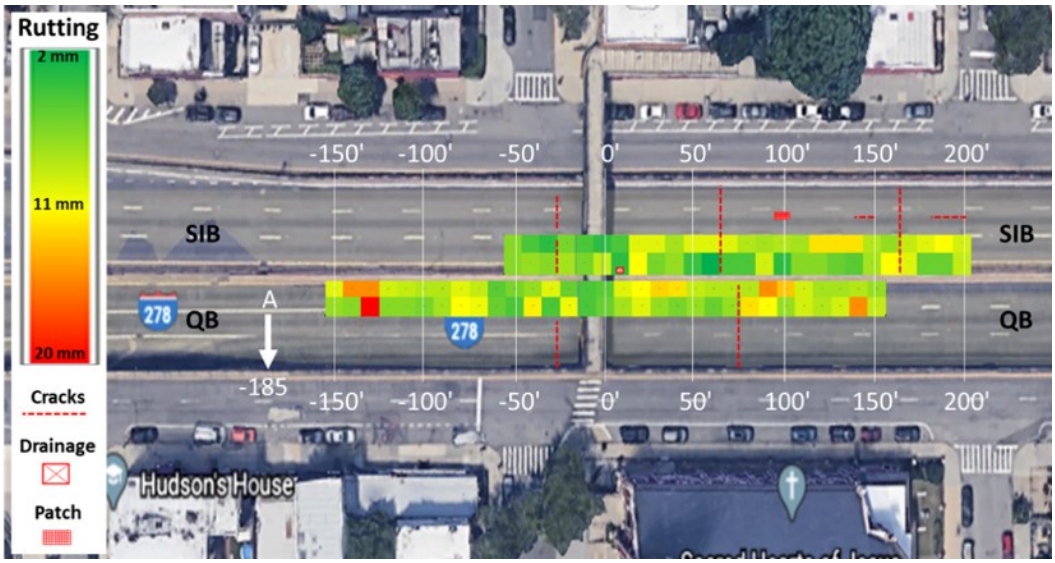

Figure 19: Roadway Survey of BQE at Summit Street

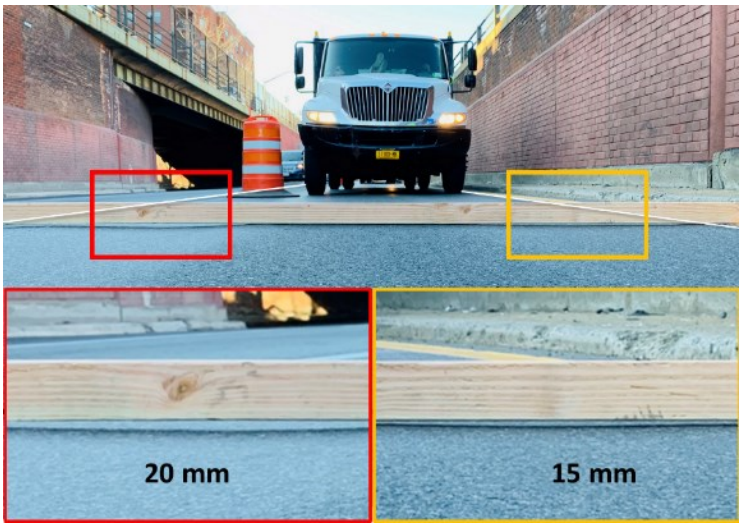

Figure 20: Maximum Rutting Depths at 140 ft prior to Pedestrian Bridge on QB

3.3.4 Recommendations for Site 1:

Based on the field survey and discussions with the Kistler representatives, the following are recommendations are made:

1. For the best outcome in terms of accuracy in GVW (i.e., less than +3%), the recommendation is to re-pave the roadway for 300 ft. in the proximity of the sensor location. Per ASTM E1318, the maximum rutting of the pavement shall be 1/8 in. 200 ft prior to and 100 ft after the sensor location. The repaving of the considered sections would provide an additional layer of confidence to achieve the accuracy and longevity of the sensors.
2. Alternatively, if the first recommendation would present delays and other constraints, it is recommended to smoothen the roadway by micro-milling the surface for 1/4-1/2 in. This process would help in minimizing the pavement rutting that will affect the accuracy of the sensors. It is worth noting that the pavement thickness after micro-milling shall be thick enough for the Quartz sensor, which requires approx. 3 in. wide and deep cut-off. It is uncertain that the exact depth of the pavement, and it is suggested to consult with the pavement program as to the last time this roadway was paved.
3. It is recommended to install the sensors before the pedestrian bridge (upstream with the traffic in each direction). The recommended sensor locations will be as follows:
    - For SIB, it is recommended to install the WIM sensors before the pedestrian bridge. Due to the several pavement defects, including drainage, cracks, patches, and rutting depth, the sections between 20 ft and 60 ft (which is between the drainage and the crack) would be the best option.
    - For QB, it is recommended to install the WIM sensors prior to the pedestrian bridge as SIB. The section should be prior to the crack at 20 ft prior to the bridge. Moreover, given that the vehicle on the ramp will be in the center of the right lane after merging into the mainline, the best section would be between -30 ft and -100 ft.

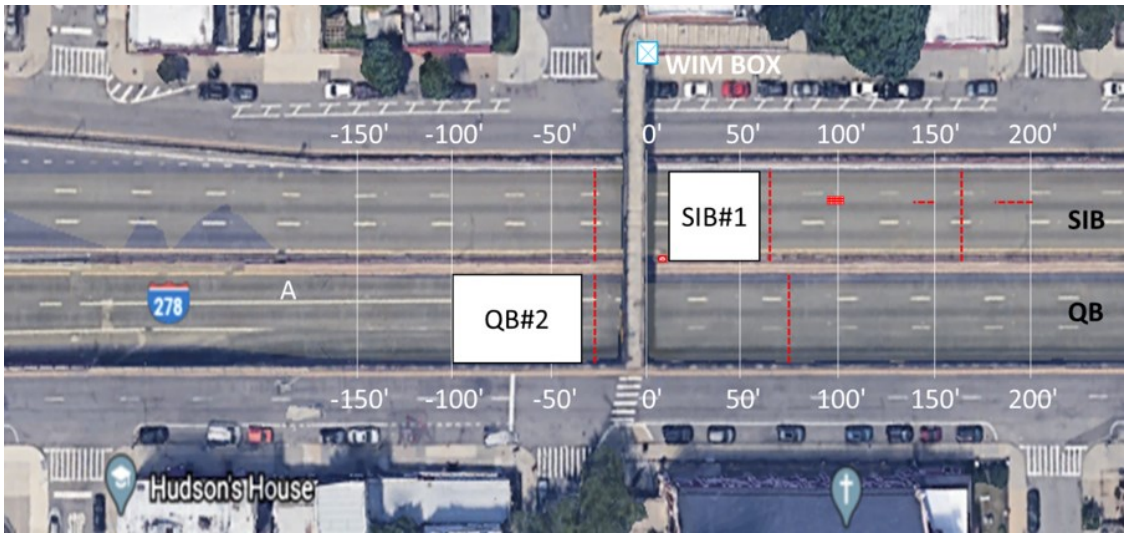

Figure 21: Recommended BQE WIM Location at Site 1

3.3.5 Review of WIM Site 2 – Pearl Street

Similarly, the roadway condition of Site 2 was also reviewed. Figure 22 shows the pavement condition excerpted from Google Earth. Figure 22(a) shows the QB pavement condition – no local rough pavement was observed, and the average slope was 3.4%. However, no cracks were found. Figure 22(b) shows the SIB condition – similar to QB, no local rough pavement was observed, the average slope was 2.2%, and no cracks were found.

Figure 23 shows the field condition of BQE Site 2. Figure 23(a) shows that two lanes (+ shoulder) were active to Queens and three lanes to Staten Island. The roadway slope was acceptable, and some rutting was observed. Figure 23(b) shows that the lanes were wider than Site 1, but it was still narrow (less than 11 ft).

(a)

(b)

Figure 22: Pavement Profile at Site 2; (a) Queens Bound (Staten Island to Queens), and (b) Staten Island Bound (Queens to Staten Island) (Reference: Google Earth)

(a) (b)

Figure 23. Field Condition at Site 2; (a) Acceptable Roughness and (b) Narrow Lane

3.3.6 Site 2 Evaluation

The team visited the second WIM site (BQE2) near Pearl Street and performed a quick survey for the Staten Island Bound (SIB) in the left lane. The team conducted an approximate measurement of pavement rutting subsidence in the left lane directly under the wheel path (approx. 1 ft. from each line stripping in the transverse direction) and the center of the lane at every 10 ft from 200 ft upstream (under the Manhattan Bridge) to 250 ft downstream (over the bridge on Adams Street) from the bridge over Pearl St in QB direction. In addition, the team measured the locations of pavement defects, such as cracks, drainages, patches, etc., of all three lanes visually.

3.3.6.1 Pavement Condition and Rutting

Table 4 summarizes the average rutting measurement of the left lane, and Figure 24 shows the roadway survey results of both the left lane (full length) and right lane (partial length). Figure 25 shows the location of the defects of BQE SIB.

Longitudinal cracks between lanes (over lane striping) are observed along the length – probably, they are the cold joints of the pavement. In the left lane, the average rutting of the left lane was 5.9 mm on both wheel paths. It was noticed that the rutting of the *left wheel path* was worse than that of the *right wheel path*. In the right lane, the rutting was estimated to be severe than the left lane. Severe pavement damage was observed at 70-90 ft. downstream from the bridge over Pearl St. Moderate rutting and cracks were observed at 140-200 ft. downstream from the bridge over Pearl St. Cracks, and patches were observed at 180-200 ft. upstream from the bridge over Pearl St. The rutting of the

downstream from the bridge over Pearl St was less than that of the upstream, and no major patches were observed.

Location	Average	Max.	Upstream Average	Downstream Average	No. of > 10 mm Rutting (Ratio, %)
Right Wheel Path	4.9 mm	14 mm	5.2 mm	4.7 mm	1 (2.5%)
Center of the Lane	3.7 mm	10 mm	3.6 mm	3.8 mm	0 (0%)
Left Wheel Path	6.8 mm	14 mm	6.9 mm	6.8 mm	1 (2.5%)
Avg. of Wheel Paths	**5.9 mm**	-	-	-	-

Table 4: Summary of Rutting Measurement of the Left Lane

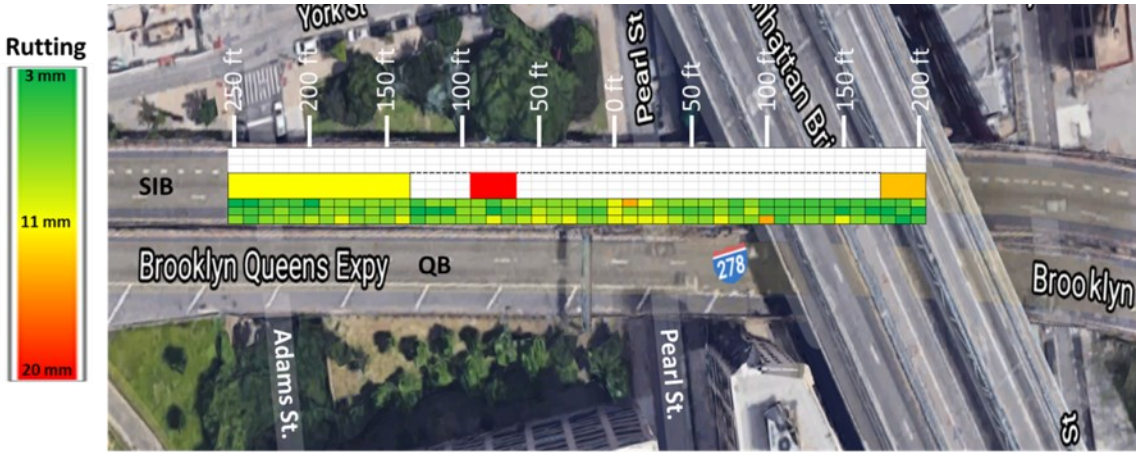

Figure 24: Roadway Survey of BQE at Pearl Street

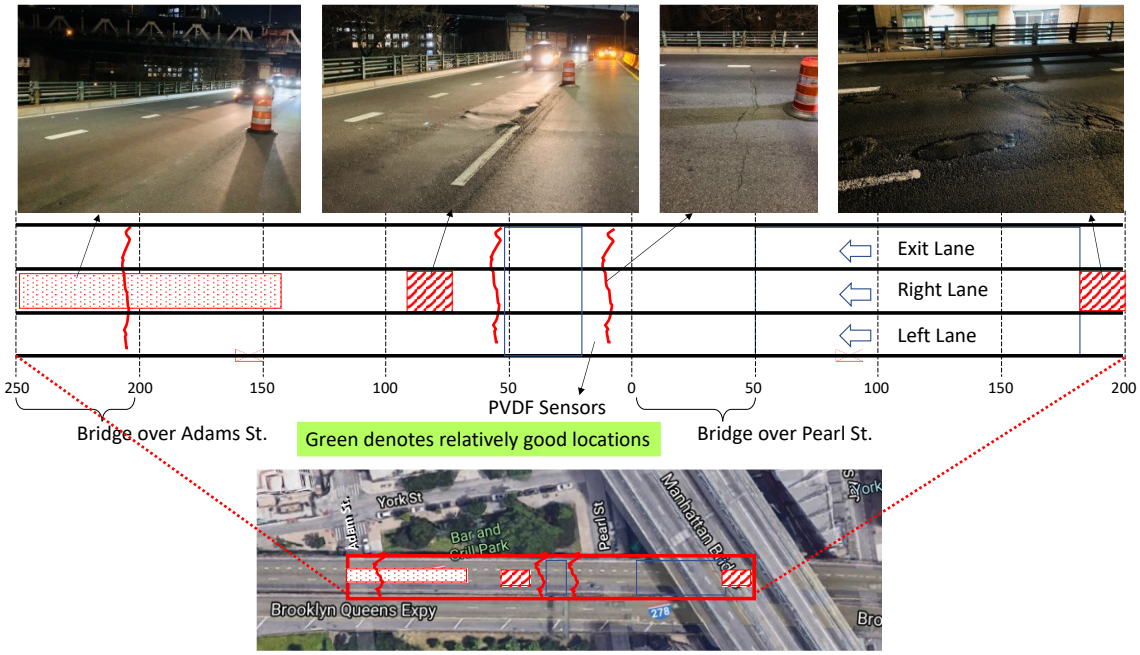

Figure 25: Roadway Survey for SIB at BQE2

3.3.6.2 Recommendations for Site 2:

Based on the field survey and discussion with the Kistler representative, the following are recommendations are made for the right lane:

1. For the best outcome in terms of accuracy in GVW and axle weights, it is highly recommended to re-pave the roadway for 300 ft. in the proximity of the sensor location. Per ASTM E1318, the maximum rutting of the pavement shall be 1/8 in. 200 ft before and 100 ft after the sensor location. The repaving of the considered sections will provide an additional layer of confidence to achieve the accuracy and longevity of the sensors.
2. Albeit the accuracy is not guaranteed based on the field condition observation, the most appropriate location in the right lane would be between 50 ft and 180 ft upstream for the Quartz sensor installation. Since the significant cracks and patches are observed at 180-200 ft. upstream, the installation location should be at least 100 ft. away from this defect to minimize the weighing error. Also, the bridge over the Pearl St. located at 0-50 ft. upstream should be avoided because the interaction between vehicle suspension and bridge would affect the accuracy. The bridge should be avoided because there is a concern with loop signals with the extra rebar reinforcing the bridge concrete that is typically used.
3. Cracks running between lanes might reduce the service life of the sensors. Water could permeate the interface between sensor epoxy and pavement, and the cables could be sheared off.
4. It is recommended to smoothen the roadway segment at 70-90 ft. downstream, where major pavement defects were observed. This smoothness would help improve the weighing accuracy and provide a safe corridor to the taxpayers.

3.4 WIM Sensor Selection

There are several different weigh-in-motion (WIM) sensor technologies, such as Piezoelectric sensor, bending plate, and load cell. The Piezoelectric sensors are subdivided into three types of sensors, Piezoceramic sensor (a ceramic material surrounded between a solid core and an outer sheath of copper), Piezopolymer sensor or PVDF (piezoelectric polymer surrounded by a flat brass casing), and Piezoquartz sensor or Lineas® Quartz sensor (quartz-sensing material placed in an aluminum alloy extrusion and covered with elastic material). In this study, PVDF sensors and Quartz sensors were used.

3.4.1 PVDF Sensor

The piezoelectric sensor converts the mechanical force applied by the tire pressure to the electric charge, which is assumed to be proportion to the tire pressure or the vehicle weight. The PVDF sensor is the most widely used because of its easy handling and installation and low price. However, this PVDF sensor does not provide good accuracy and long service life. The PVDF sensor has a dynamic character because the charges are generated only when it is forced; therefore, it is not applicable to estimate the static vehicle at very low speed (less than 10 mph) like the load cell. In addition, the PVDF sensor is very susceptible to the change in environmental conditions, such as the pavement roughness, vehicle's dynamic suspension, pavement materials, pavement, and ambient temperature, etc. (Nassif et al., 2018). These limitations will produce inherent errors; however, they could be minimized by selecting the proper WIM sites (error due to roughness, vehicle suspension, and pavement material) and compensating the WIM data (error due to pavement and ambient temperature). The service life of the PVDF sensor is generally 3-4 years, depending on the severity of the weather. The majority of sensors are ripped off while plowing the snow during winter in the northeast region. The estimated annum costs with a discount rate of 10 % over 20 years are $3,092 ~ $5,000 (Mimbela et al., 2000; Bushman et al., 1998; Zhang, 2007).

3.4.2 Quartz Sensor

Piezoquartz or Quartz sensor is another Piezo-type sensor as PVDF and emerging technology in Piezo-type sensor. Unlike the PVDF sensor, the Quartz sensor is insensitive to temperature and force direction, and therefore, it is more accurate than the PVDF sensor. The accuracy of the Quartz sensor is comparable to the Load Cell. Quartz sensors are sensitive to forces in the vertical direction. Still, they are not susceptible to forces in the horizontal direction due to vehicle inertia because Quartz sensors are encased in an aluminum alloy extruded profile. Although Quartz sensors are more expensive, they provide better accuracy and are more reliable in estimating vehicle weights than PDVF sensors because they are insensitive to temperature variation and force direction. The service life of the Quartz sensor is not well defined because they have been recently developed, but manufacturers claim that it will last

more than 15 years. The Quartz sensor can provide an accuracy of ±10%/GVW with 100% confidence (Zhang, 2007).

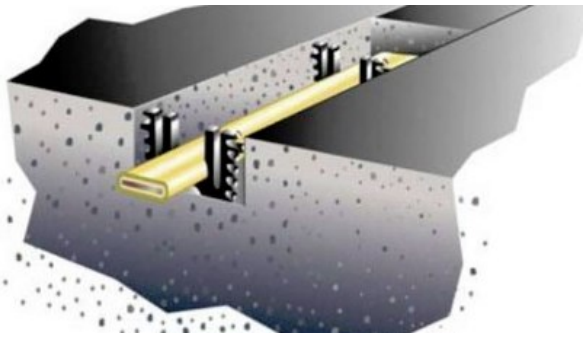

Figure 26: PVDF Sensor

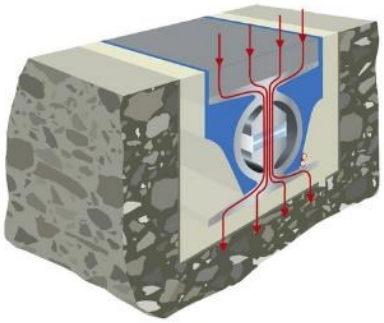

Figure 27: Quartz Sensor

3.4.3 Load Cell Sensor

The single load cell sensor utilizes a dynamic rated load cell to measure the vehicle weight that is embedded in an enclosure covered by a rigid steel plate. The wheel force directly presses the single load cell that is proportional to the vehicle weight. The load cell does not have any inherent error due to temperature and pavement type because the load cell is encased with solid material. Such encasement provides good accuracy, and the load cell provides the most accurate weight data compared to PVDF and Bending Plate. The tolerance of gross vehicle weight of the single load cell is within ±6% of the actual vehicle weight. However, the load cell requires a huge cut of pavement, and therefore, it is the most expensive for installation and maintenance among all types of sensors. The estimated annum cost is reported to be $5,982~$8,300 with a 10% discount rate over 20 years (Mimbela et al., 2000; Bushman et al., 1998; Zhang, 2007).

Figure 28: Load Cell and Installation Example

3.4.4 Bending Plate Sensor

The bending plate is encased with solid material covered by a steel plate. Therefore, the bending plate is not affected by the temperature or other environmental conditions, similar to the load cell. The bending plate utilizes the strain gauge to measure the vehicle load attached to the underside of the steel plate. The principle of bending plate is when the steel plate is distorted by the vehicle, a strain signal is transmitted to the WIM system proportional to the vehicle load. This sensor is less expensive than the single load cell but provides equivalent accuracy within 10% tolerance. The accuracy and installation cost of bending plate WIM system falls between PVDF sensor and load cell WIM system. The estimated annum cost falls between $4,636 and $6,400 (Mimbela et al., 2000; Bushman et al., 1998; Zhang, 2007).

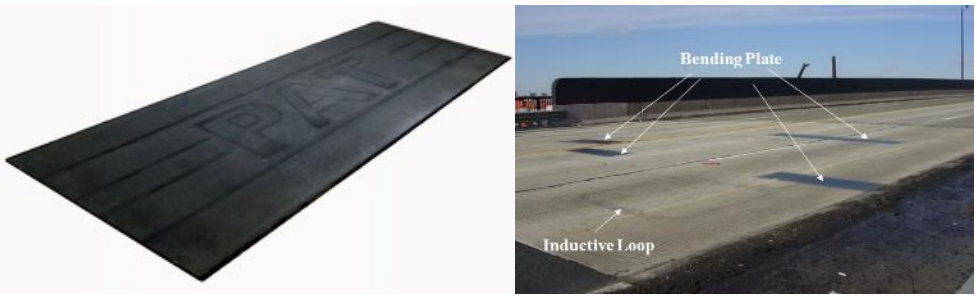

Figure 29: Bending Plate and Installation Example

3.4.5 Inductive Loop

The preformed Sawcut Style Loop consists of a non-spliced and machine-twisted lead-in copper wire insulated with a cross-linked polypropylene jacket. The inductive loop is installed into a slot in the roadway for permanent application. When a vehicle moves over the loop, the resonate frequency will change as a magnetic field in the loop area changes. A closed-loop 6 ft x 6 ft loop with 100 ft of cable was used for this project, as shown in Figure 30.

Figure 30: Pre-sawcut Loop

3.5 WIM Installation

3.5.1 WIM Sensor Layout for BQE Site 2

Two PVDF sensors and one loop were installed on each lane. Two PVDF sensors were distanced at 12 ft, and a loop with 6 ft. x 6 ft was installed in the center between two PVDF sensors. Each PVDF sensor will be 10 ft. or 11 ft., depending on the lane width. One PVDF sensor will measure the axle weight independently from another PVDF sensor, and the average of both PVDF sensors will be the axle weight for a given vehicle. The timestamp and known distance between two PVDF sensors will be used to determine the speed and axle spacing. Thus, the PVDF sensors will identify the axle weight and axle spacing, and the loop will identify the presence of each vehicle. Both sensors will be used to classify the vehicle per FHWA classification.

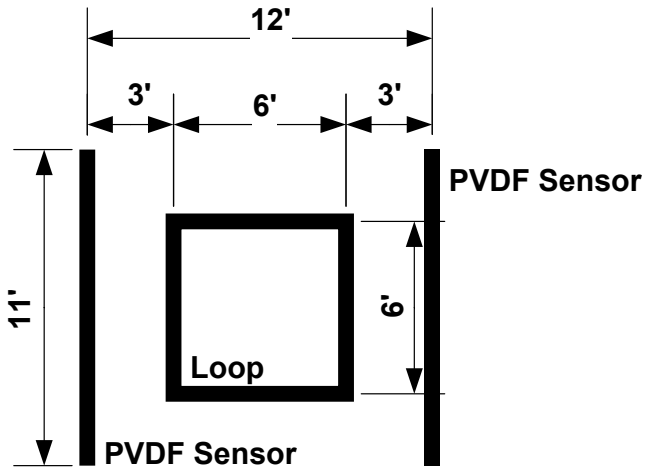

Figure 31: Typical PVDF and Loop Layout

Four Quartz sensors and two loops were installed on the right lane of BQE QB. The team obtained the average speed at BQE, and Table 5 summarizes the average vehicle speed at peak hours. The team reviewed and discussed the speed data, site geometry, and pavement condition with the Kistler representative and determined the Quartz sensor layout as depicted in Figure 32. As can be seen in Figure 32, the sensor layout is different from the PVDF layout, and the Quartz sensors are zig-zagged distributed. This layout will help improve the axle weight, axle spacing, and speed accuracy when the vehicles are bumper-to-bumper because it has 4 independent readings at 4 distinct time stamps. Figure 33 shows the final layout of WIM sensors at BQE Site 2 near Pearl Street.

Average Speed (MPH)		Peak Hour	
Location	**Direction**	**AM**	**PM**
South of Atlantic Ave (Site 1)	Queens Bound	17.5	10
	Staten Island Bound	29	11
North of Brooklyn Bridge (Site 2)	Queens Bound	37.5	12.22
	Staten Island Bound	29.5	9.5

Table 5: Average Speed at BQE WIM Sites

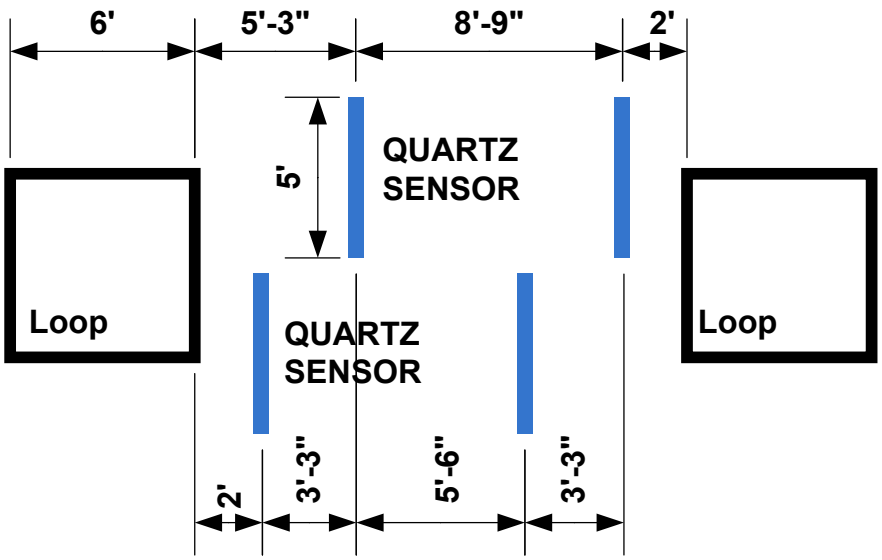

Figure 32: Typical Quartz and Loop Layout

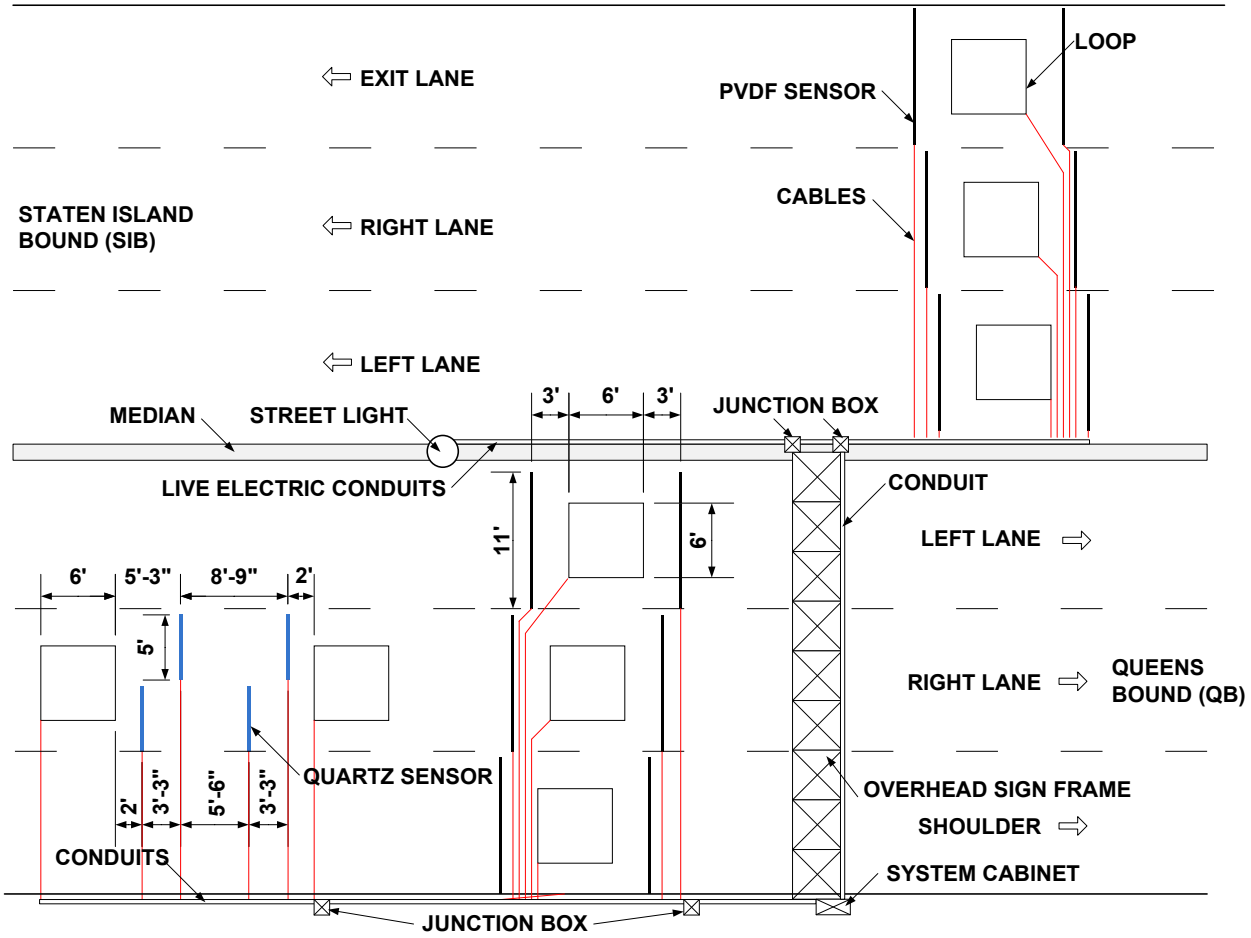

Figure 33: Final WIM Sensor Layout at BQE Site 2

3.5.2 WIM Installation Procedure

The WIM installation was performed for 3 consecutive nights between September 27, 2019, and September 30, 2019, from 10-11 pm to 5-6 am of the next day. The contractor cut, cleaned, and dried the slots for the WIM installation. Figure 34 shows the dimension of each slot for PVDF, Quartz, and Loop. In the meantime, the team prepared and cleaned the sensors and installed the sensors in the slots when the slots were dried entirely. Then the contractor poured the epoxy and finished the installation. Steps are summarized below, and Figure 36 summarizes the field pictures for each step.

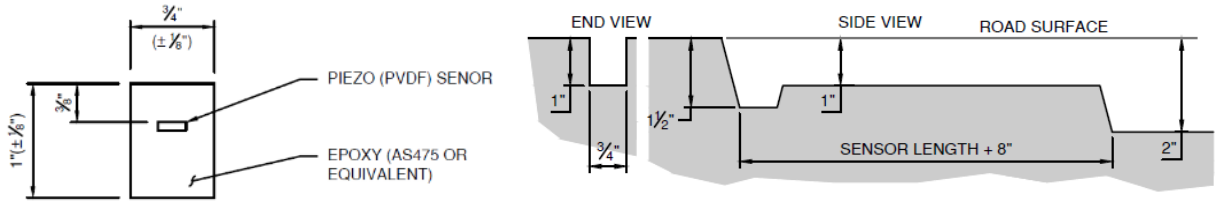

(a)

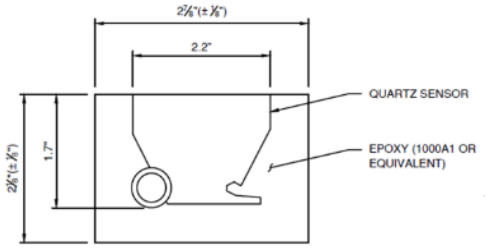

(b)

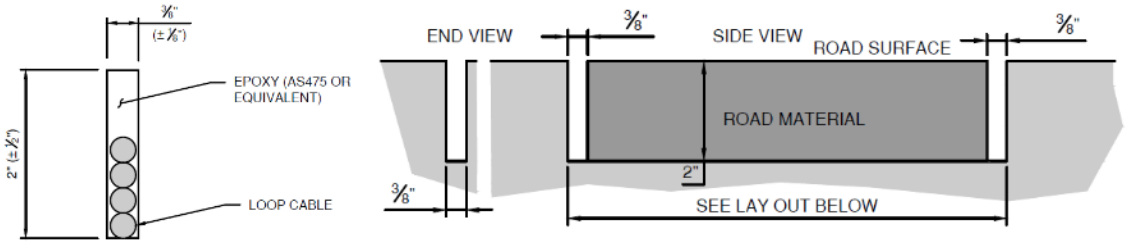

(c)

Figure 34: Slot Configuration; (a) PVDF, (b) Quartz, and (c) Loop Cables

1) Determine the actual location depending on the review of on-site pavement condition. Draw the sensor locations using a rope and white spray per specification. The dimensions shall meet the specification requirement within tolerance. The sensors shall be perpendicular to the traffic flow and the sensor shall be located in the center of each lane. Drawing for cables may be combined, but drawings for sensors shall not be overlapped. Minimize or eliminate any drawing angle less than a right angle, which may damage the cable during operation.

2) Cut the pavement for the WIM sensor slots using the saw-cutting machine. PVDF sensor slot shall be 3/4 in. wide, 1 in. deep, and 11 ft-8 in long for 11 ft PVDF sensor (10 ft-8 in. long for 10 ft PVDF sensor). The width shall not exceed 1 in. Quartz sensor slot shall be 2-7/8 in. wide, 2 in. high, and 5 ft long. Home run slot for cables shall be 1/4 in. wide, 1.5~2.0 in. deep depending on the pavement thickness

and long enough to reach the parapet. After cutting, clean and dry all slots with pressurized air to remove all dirt, debris, and water. Duct tape along the sides of the WIM sensor slots.

3) For PVDF sensors, wipe WIM sensors using cloths soaked with alcohol. Place installation brackets on the sensor at an interval of 6 in. throughout its length. Place the sensor with brackets and/or cables into the cut slot and check the sensor depth with a depth gauge. Please note that PVDF sensors will be installed before pouring. For Quartz sensors, test sensors using the instrument provided by Kistler – insulation resistance test, ground test, and capacitance test. Tie two wood pieces included in the Quartz sensor package and place the sensor next to the slot. Please note that the Quartz sensor will be installed after pouring. Place the loop and cables into the cut slot, and push them into the bottom of the slot.

4) For AS475 (PVDF epoxy), mix the large container of the grout to be homogenous without any lumps using an electric drill (at 450 to 550 rpm) and a mixing paddle. Add the hardener to the grout and mix another minute. The amount of hardener depends on the ambient temperature, as summarized in Table 6. Pour the grout mixture over the sensors, loops, and cables, and spread the grout smooth to make the grout slightly higher (1/16 in.) than duct tape. Remove duct tape before the final set of the grout (5~10 minutes after grouting), and cure the grout for at least 45 minutes depending on the ambient temperature. For 1000A1 (Quartz epoxy), take the resin and hardener, and pour the resin (plastic canister) into the original bucket, followed by hardener in a can. Mix the resin and hardener thoroughly with a heavy-duty mixer with adjustable speed. During mixing, pour the sand into the mixture gradually to avoid lumps forming. Pour the grout mixture into the slot and then place the sensors. If needed, use the kerosene forced air heater to accelerate the grout curing. If needed, use an angle grinder to grind the excessive grout to make the surface smooth.

Temperature	Benzoyl Peroxide Organic (BPO) Powder	
°C (°F)	To Mix 9 Kg of Grout	To Mix 18 Kg of Grout
< 13 (55)	3 X 33g Vials	6 X 33g Vials
13 – 24 (55-75)	2 X 33g Vials	4 X 33g Vials
> 24 (75)	1 X 33g Vials	2 X 33g Vials

Table 6: AS475 Accelerator Dose Table

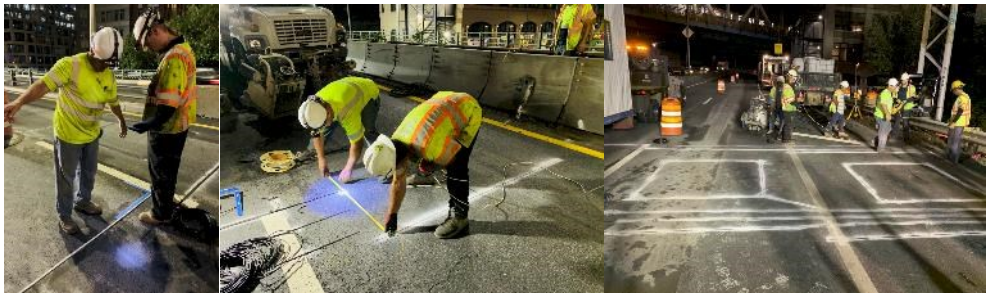

(a)

(b)

Figure 35: WIM Sensor Instrumentation; (a) Layout Drawing, and (b) Sawcutting/Cleaning

(a)

(b)

Figure 36: WIM Sensor Instrumentation Procedure; (a) PVDF Sensor and (b) Quartz Sensor

3.6 WIM Calibration Test

A calibration test for the BQE WIM site was performed on Monday, 9/30/2019, between 10 pm and 4 am of the next day. A Class 9 truck (5-axle, Type 3S2 split) with a flatbed was hired for this task. Three concrete blocks were tied and fixed on the flatbed as weighing material to minimize the load movement during calibration.

3.6.1 Calibration Procedure

The procedure is that a truck with known GVW and axle weights (calibration truck) runs over the WIM sensors multiple times to determine the sensor factors. Below is the typical step-by-step calibration procedure.

- The calibration truck should be the same type and/or configuration in which the owners are the most interested. In general, 3- or 4-axle single unit truck (FHWA Class 6 or Class 7) or 5-axle semi-tractor trailer (FHWA Class 9) is used for calibration.

- On the day of the calibration test, the truck shall be loaded in an open-box bed (Class 6 or Class 7) or on the trailer bed (Class 9), so that the GVW with load will be at least 60 kips and preferably close to 80 kips. The most appropriate type of load is a heavy, fixed, and divisible load that is stable and immovable during calibration test. For FHWA Class 9 truck, concrete blocks or a similar type of load would be appropriate. For Class 6 or Class 7, the larger and denser aggregate would be appropriate rather than sand or smaller aggregate, as larger and denser aggregates are more stable than others during the calibration test.

- The calibration truck shall be measured at a certified static scale to measure the gross vehicle weight and "each" individual axle weight. Some contractors may argue that it is not practical to measure individual axle weight because the axle spacing within tandem or tridem is too close. In such a case, the tandem or tridem can be measured together and divide by the number of axles. Below is the typical weighing procedure with tandem for Class 9 Truck and summarized in Figure 37.

    - Measure the front axle weight (W1) – Figure 37(a)

    - Measure the front axle weight and (Wa) – Figure 37(b)

    - Measure the gross vehicle weight (GVW) – Figure 37(c)

    - Measure the tandems of tractor and trailer (Wb) – Figure 37(d)

    - Measure the tandem of the trailer (Wc) – Figure 37(e)

- The truck driver shall provide all the weight certificates to the engineers for calibration. Each axle weight can be determined as below. Each axle weight will be adjusted so that the summation of axle weight is the GVW.

    - Front axle weight = average of (W1) and (GVW-Wb)

    - Each axle of tractor tandem = average of (Wa-W1) and (GVW-Wc-W1)

    - Each axle of trailer tandem = average of (GVW-W1) and (Wc)

- The engineers for calibration shall measure the axle spacing between axles and overall wheelbase and length. In addition, the overhang (from front bumper to front axle), underhang

(from rear bumper to rear axle), and front and rear track width can be measured. Figure 42 shows an example of calibration truck dimensions.

- The calibration truck shall run multiple times over each lane where the WIM sensors are installed. During running, the truck shall maintain in the middle of the lane to maximize the signal strength. When passing over the sensors, the truck shall maintain its speed constantly (no acceleration nor break). The number of runs will be determined by the engineers for calibration. Figure 43 shows an example of a calibration run.

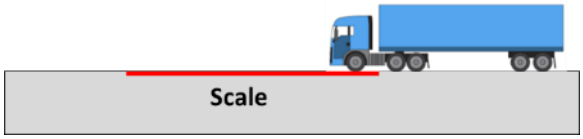

Figure 37a: Calibration Truck Weighing Procedure (W1)

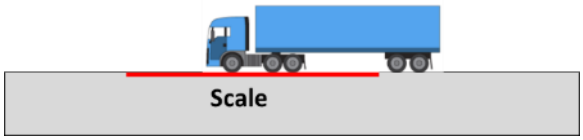

Figure 38b: Calibration Truck Weighing Procedure (Wa)

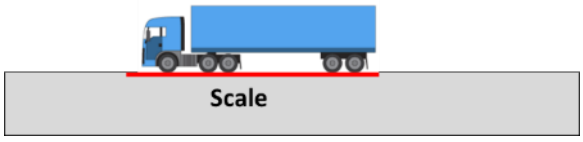

Figure 39a: Calibration Truck Weighing Procedure (GVW)

Figure 40a: Calibration Truck Weighing Procedure (Wb)

Figure 41a: Calibration Truck Weighing Procedure (Wc)

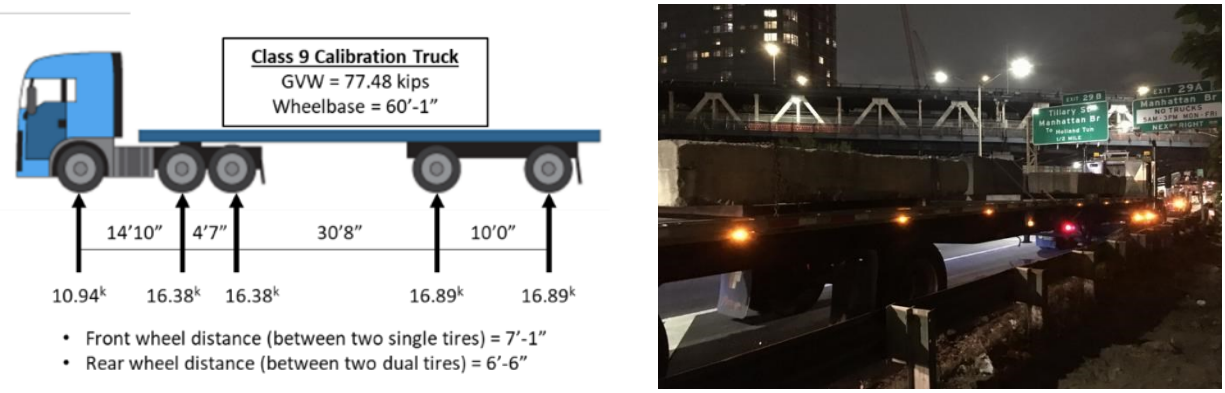

Figure 42: Calibration Truck

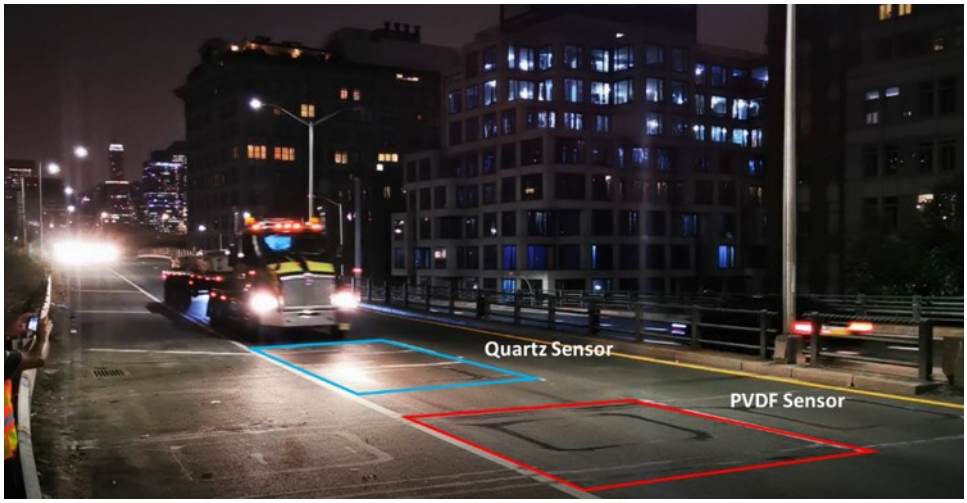

Figure 43: Calibration Test at BQE WIM

3.6.2 Calibration Results for Staten Island Bound (SIB)

PVDF Sensor in Lane 1 (Right Lane)

This is the exit lane to Old Fulton Street. A total of 4 runs were made, and the results were consistent between runs. The gross vehicle weight (GVW) errors between runs were -4.7% ~ 2.4%, and the average absolute error was 2.5%. The final sensor factors are 2.61 for sensor 1 (upstream) and 2.19 for sensor 2 (downstream). The results are summarized in Table 7.

PVDF Sensor in Lane 2 (Center Lane)

This is the center lane where the majority of the trucks would travel in SIB of the BQE. A total of 6 runs were made, and the GVW errors were between -7.2% and 8.1%, and the average absolute error was 4.7%. For all the cases, the results are consistent between runs, and the GVW error was within 10% of the calibration truck GVW. The final sensor factors are 1.82 for sensor 1 and 2.62 for sensor 2. The results are summarized in Table 8.

PVDF Sensor in Lane 3 (Left Lane)

This is the left thru traffic lane. A total of 7 runs were made, and the GVW errors were -4.4% (minimum) ~ 6.7% (maximum). The average absolute error was 3.5% which is less than 10%. The results are consistent between runs. The final sensor factors are 2.60 for sensor 1 and 2.78 for sensor 2. The results are summarized in Table 9.

Run #	Target GVW (lb)	Sensor 1 Factor	Sensor 2 Factor	Factored GVW (lb)	Error (%)
1	77,480	2.52	2.16	79,360	2.4%
2	77,480	2.48	2.24	78,567	1.4%
3	77,480	2.69	2.06	78,725	1.6%
4	77,480	2.74	2.30	73,801	-4.7%
Average	**77,480**	**2.61**	**2.19**	**77,613**	**2.5%**
Std. Dev. (COV)		**0.11 (4.2%)**	**0.09 (4.1%)**	**2,221 (2.9%)**	

Table 7: Calibration Results for SIB-RL

Run #	Target GVW (lb)	Sensor 1 Factor	Sensor 2 Factor	Factored GVW (lb)	Error (%)
1	77,480	1.91	2.57	76,402	-1.4%
2	77,480	1.63	2.51	83,771	8.1%
3	77,480	1.88	2.75	74,506	-3.8%
4	77,480	2.15	2.60	71,880	-7.2%
5	77,480	1.66	2.64	81,007	4.6%
6	77,480	1.68	2.68	79,694	2.9%
Average	**77,480**	**1.82**	**2.62**	**77,888**	**4.7%**
Std. Dev. (COV)		**0.18 (9.9%)**	**0.08 (3.1%)**	**4,037 (5.2%)**	

Table 8: Calibration Results for SIB-CL

Run #	Target GVW (lb)	Sensor 1 Factor	Sensor 2 Factor	Factored GVW (lb)	Error (%)
1	77,480	2.36	2.69	82,667	6.7%
2	77,480	2.52	2.60	81,329	5.0%
3	77,480	2.63	2.69	78,379	1.2%
4	77,480	2.64	2.97	74,495	-3.9%
5	77,480	2.64	3.00	74,078	-4.4%
6	77,480	2.71	2.76	76,236	-1.6%
7	77,480	2.70	2.76	76,366	-1.4%
Average	**77,480**	**2.60**	**2.78**	**77,650**	**3.5%**
Std. Dev. (COV)		**0.11(4.2%)**	**0.14 (5.0%)**	**3,061 (3.9%)**	

Table 9: Calibration Results for SIB-LL

3.6.3 Calibration Results for Queens Bound (QB)

PVDF Sensor in Lane 1 (Shoulder Lane)

This lane is the shoulder and is not for traffic; however, the sensors are installed for future usage. A total of 3 runs were made. The results were not consistent between runs because of the drain grate and uneven pavement. The minimum and maximum GVW errors were -11.1% and 11.8%, respectively, and the average absolute error was 9.0%. The error extent was greater than the other two

lanes. The final sensor factors are 2.37 for sensor 1 and 1.96 for sensor 2. The results are summarized in Table 10.

PVDF Sensors in Lane 2 (Right Lane)

This is the main lane for trucks that will exit onto the Manhattan Bridge or pass to the Flushing Queens. A total of 5 runs were made to determine the calibration factors. The results were not as consistent between runs compared to SIB direction. The minimum and maximum errors were -17.6% and 7.6%, respectively, and the average absolute error was 8.6%. The results are summarized in Table 11.

PVDF Sensors in Lane 3 (Left Lane)

This is the left thru traffic lane to Flushing, Queens. Five runs were made to determine the calibration factors of the PVDF sensors. The results were not consistent between runs. The GVW errors were -26.0% ~ 26.1%, which was much higher than the SIB lanes. Thus, the average absolute error was 19.3%. The results are summarized in Table 12

Run #	Target GVW (lb)	Sensor 1 Factor	Sensor 2 Factor	Factored GVW (lb)	Error (%)
1	77,480	2.13	1.74	86,626	11.8%
2	77,480	2.63	2.19	68,910	-11.1%
3	77,480	2.42	2.04	74,369	-4.0%
Average	**77,480**	**2.37**	**1.96**	**76,635**	**9.0%**
Std. Dev. (COV)		**0.20 (8.4%)**	**0.20 (10.2%)**	**7,408 (9.7%)**	

Table 10: Calibration Results for QB-SH

Run #	Target GVW (lb)	Sensor 1 Factor	Sensor 2 Factor	Factored GVW (lb)	Error (%)
1	77,480	1.21	1.77	70,143	-9.5%
2	77,480	1.40	1.85	63,867	-17.6%
3	77,480	1.04	1.51	82,013	5.8%
4	77,480	1.08	1.55	79,458	2.6%
5	77,480	1.03	1.47	83,404	7.6%
Average	**77,480**	**1.14**	**1.60**	**76,985**	**8.6%**
Std. Dev. (COV)		**0.21 (18.4%)**	**0.23 (14.4%)**	**12,123 (15.7%)**	

Table 11: Calibration Results for QB-RL

Run #	Target GVW (lb)	Sensor 1 Factor	Sensor 2 Factor	Factored GVW (lb)	Error (%)
1	77,480	1.00	0.97	93,289	20.4%
2	77,480	0.96	0.92	97,698	26.1%
3	77,480	1.59	1.62	57,324	-26.0%
4	77,480	1.41	1.44	64,567	-16.7%
5	77,480	1.28	1.29	71,587	-7.6%
Average	**77,480**	**1.19**	**1.23**	**74,467**	**19.3%**
Std. Dev. (COV)		**0.23 (19.3%)**	**0.27 (22.0%)**	**15,499 (20.8%)**	

Table 12: Calibration Results for QB-LL

3.6.4 Calibration Results for Quartz Sensors in Lane 2 (Right Lane)

In the right lane of the BQE QB direction, four Quartz sensors were installed in addition to the PVDF sensors. Each Quartz sensor was calibrated to determine the sensor calibration factor. The results were very consistent between runs, and the minimum and maximum GVW errors were -5.1% and 1.5%, respectively. The average absolute GVW error was 1.67%. The results are summarized in Table 13.

Run #	Target GVW (lb)	Sensor 1 Factor	Sensor 2 Factor	Sensor 3 Factor	Sensor 4 Factor	Factored GVW (lb)	Error (%)
1	77,480	1.130	0.891	1.087	0.966	78,460	1.3%
2	77,480	1.037	0.989	1.024	1.028	78,480	1.3%
3	77,480	0.957	1.018	0.970	0.999	76,080	-1.8%
4	77,480	1.009	1.004	0.969	0.999	76,760	-0.9%
5	77,480	1.016	1.016	1.022	1.014	78,460	1.3%
6	77,480	1.016	0.994	1.046	1.003	78,320	1.1%
7	77,480	0.950	1.027	0.997	0.986	76,380	-1.4%
8	77,480	0.910	1.007	0.911	0.986	73,500	-5.1%
9	77,480	1.060	0.964	1.048	1.007	78,660	1.5%
10	77,480	0.981	1.026	0.961	1.012	76,700	-1.0%
Average	**77,480**	**1.007**	**0.994**	**1.004**	**1.000**	**77,180**	**1.67%**
Std. Dev. (COV)		**0.059 (5.9%)**	**0.039 (3.9%)**	**0.049 (4.9%)**	**0.016 (1.6%)**	**1,557** (2.0%)	

Table 13: Calibration Results for QB-RL with Quartz Sensors

4. Evaluation of WIM Data Quality

4.1 Quality Assurance of WIM data from BQE Site

Dahlin (1992) offered a practical method to calibrate a WIM system explicitly based on the steering axle weights (or front axle weights, FAW) and gross vehicle weights (GVW) of FHWA Class 9 trucks. They used the FAW and GVW data produced by the sensors to control any drifts from various parameters such as climate and traffic conditions. They confirmed bimodal distribution validated GVW, and FAW by the average steering axle weight per three GVW categories.

Ott and Papagiannakis (1996) discussed issues with the method of Dahlin, indicating that since the estimated GVW of 3S2 trucks was summations of weight estimations of the axles, the error of GVW estimation would be lesser than the error of estimate for each axle. This is because each axle weight could diminish the errors in the GVW. Also, the method is based on the distribution of GVW and does not consider other factors. They performed extensive analyses for static data of the 3S2 trucks (GVW and FAW) from 976 sites and showed that close to 80% of the sites had bimodal load patterns (including two peaks for unloaded and loaded trucks), 14% unimodal (loaded), 4% unimodal (unloaded), and 2% multimodal (more than two peaks).

Several studies have been performed specifically for WIM data quality control and quality assurance (Southgate, 2001; Wei et al., 2003; Nichols et al., 2004; Turner, 2007; and Monsere et al., 2008). For instance, Nichols et al. (2004) proposed a WIM data quality control (QC) method to check axle spacing and weight accuracy using FAW and drive tandem axles of 3S2 trucks.

Two systems are running on the BQE WIM sites. The WIM data from Quartz sensors are collected from October 3rd, 2019, for Queens Bound (QB), while the WIM data from PVDF sensors are collected from October 16th, 2019, and October 11th, 2019, for QB and Staten Island Bound (SIB), respectively. WIM data are processed using the filters from NCHRP 12-83 to take out the wrong readings and car records. The following analysis results of quality assurance were based on the WIM data from the beginning to December 2nd, 2019.

After the WIM data were filtered as recommended by NCHRP 12-83, additional quality assurance was performed. The most relevant work on validating the WIM data is the methodology performed by Southgate. In this well-known approach, he used the front axle weight (FAW) of FHWA Class 9 truck (3S2, semi-tractor trailer) to calibrate the WIM data using a logarithmic regression because the properties of the steering axle are mainly related to the drive tractor and not the payload. The author used these Class 9 3S2 type trucks because they are standard commercial trucks and because they have a stable relationship between the FAW and the steering axle spacing. He established a logarithmic relation between those two variables and used this relation to adjust WIM data. This

technique uses the relationship between the first axle spacing (S12) and the ratio between steering axle weight and first axle spacing (A1/S12). If the regression curve of all Class 9 falls within the upper and the lower boundary and close to the reference equation, then the quality of WIM data is acceptable.

Figure 44 shows the Southgate regression curves for BQE WIM sites – IRD denotes the data collected by the IRD system and PVDF sensors, and Kistler denotes the data collected by the Kistler system and Quartz sensors. The Purple sold curve is the lower boundary, and the solid orange curve is the upper boundary, indicating the maximum steering axle weight to the spacing ratio by manufacturers' specifications. The solid green curve is the reference line that falls between lower and upper boundaries. The red dash curve is the regression curve of each site and year, and blue dots are each data point of Class 9 truck. the lower cut-off for blue dots is occurred by one of the NCHRP 12-83 filter (minimum axle weight = 2 kips). Some results over 2000 in y-axle (FAW/S12) are also cut-off for better visualization. The results also indicate that the dispersion is reasonable, and the data quality is confirmed.

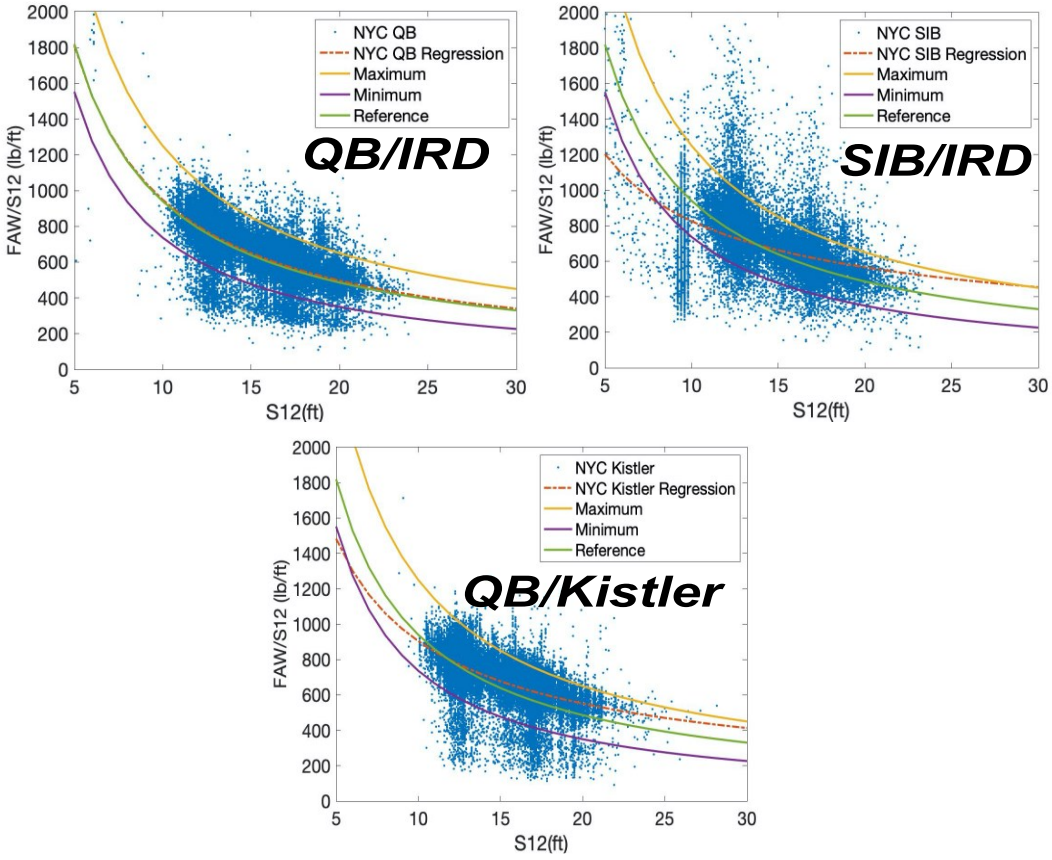

Figure 44: Southgate Regression Curve for BQE Site

Figure 45 summarizes the distribution of GVW of Class 9 trucks compared to QB/Kistler data which would provide the most accurate data. For QB and SIB, albeit the GVW is biased to heavier weight. Figure 46 summarizes the distribution of FAW of Class 9 trucks compared to QB/Kistler data.

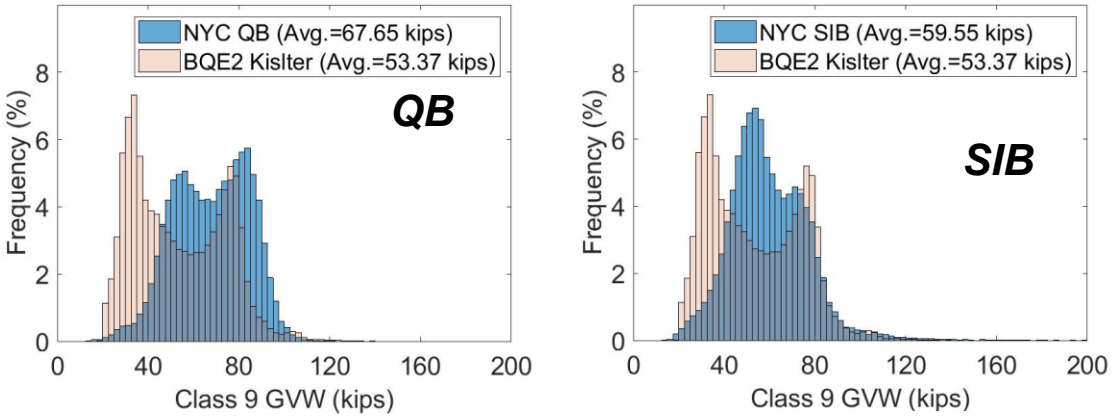

Figure 45. Comparison of the GVW of Class 9 Trucks

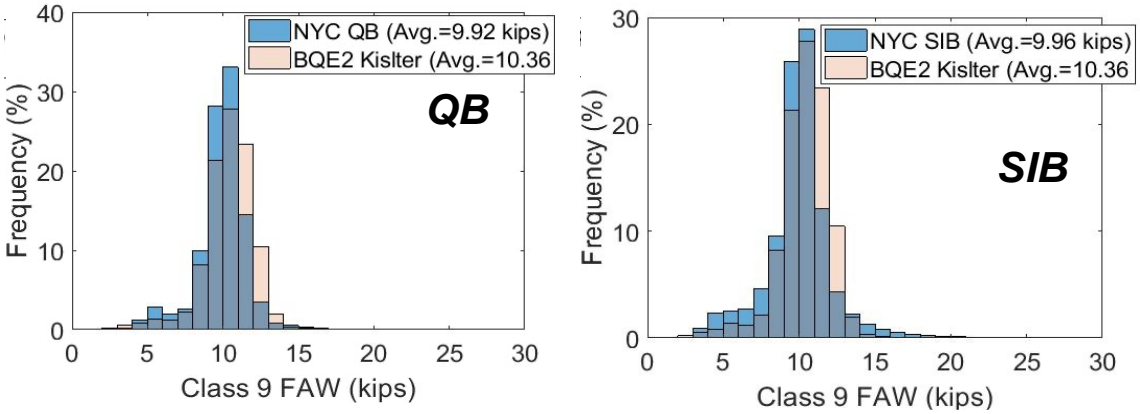

Figure 46: Comparison of the Front Axle Weight of Class 9 Trucks

4.2 Truck Statistics of WIM Data

Traffic statistics from the BQE site are summarized in Table 14. Figure 47 and Figure 48 show the distributions of GVW on QB-IRD and SIB-IRD, respectively. Figure 49 and Figure 50 show the distribution of vehicle classifications and lanes, respectively, for IRD data. Figure 51 shows the number of trucks above 150 kips per day. Both directions of BQE have ADTT of around 5,000. Although QB has more overweight trucks percentage and volume per Federal Bridge Formula (FBF), SIB has more heavy trucks (above 150 kips). The number of trucks over 150 kips decreased significantly after November 20th, 2019.

WIM System	Period	No. of Days	Total Counts	Truck Counts	% Truck Traffic	ADTT	Illegal OW	OW per FBF	OW %	Daily OW
QB (Kistler) Right lane only	10/02/19-12/04/19	61	1,671,845	229,944	14%	3,770	23	33,956	15%	557
QB (IRD)	10/16/19-12/04/19	50	2,793,570	244,900	9%	4,898	1	66,828	27%	1,337
SIB (IRD)	10/11/19-12/04/19	55	3,259,393	288,500	9%	5,245	596	36,119	13%	657

Table 14: Statistics of Traffic from BQE Site

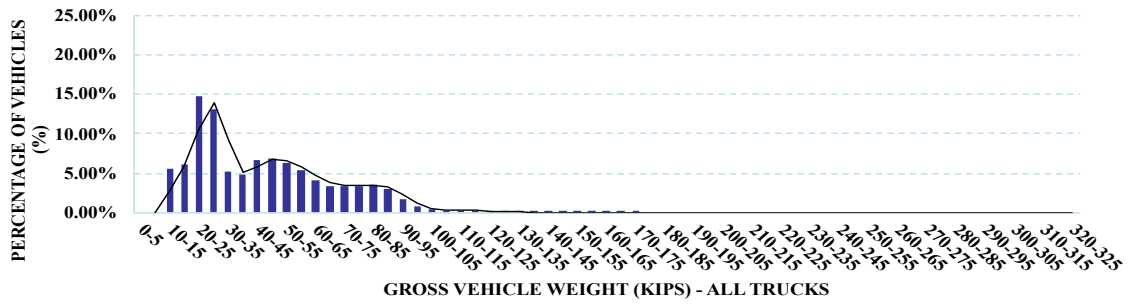

(a)

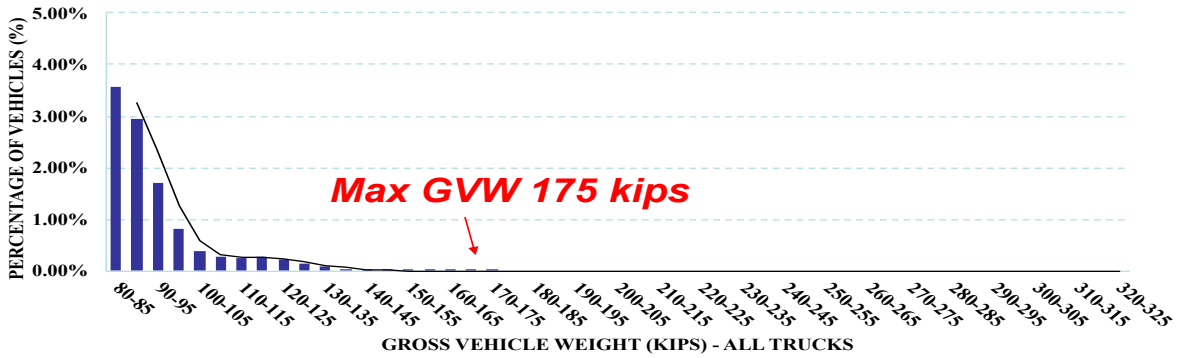

(b)

Figure 47: Distribution of GVW for QB (IRD) data; (a) All GVW Ranges, and (b) OW Only

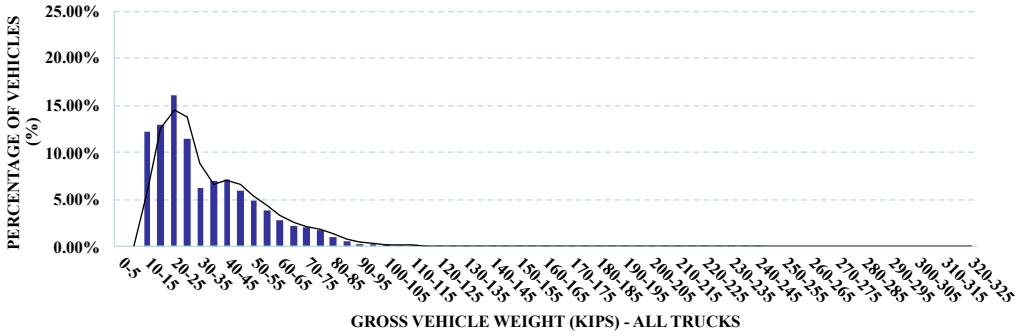

(a)

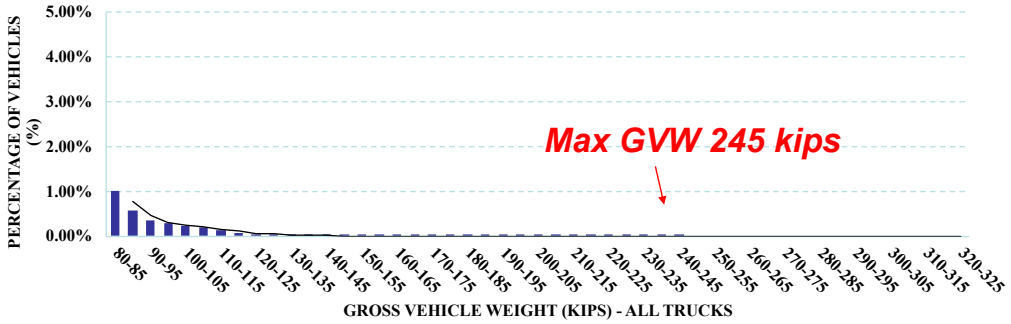

(b)

Figure 48. Distribution of GVW for SIB (IRD) data; (a) All GVW Ranges, and (b) OW Only

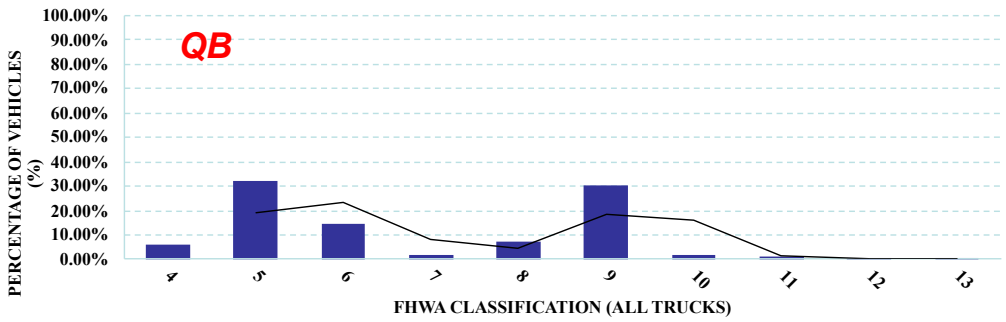

(a)

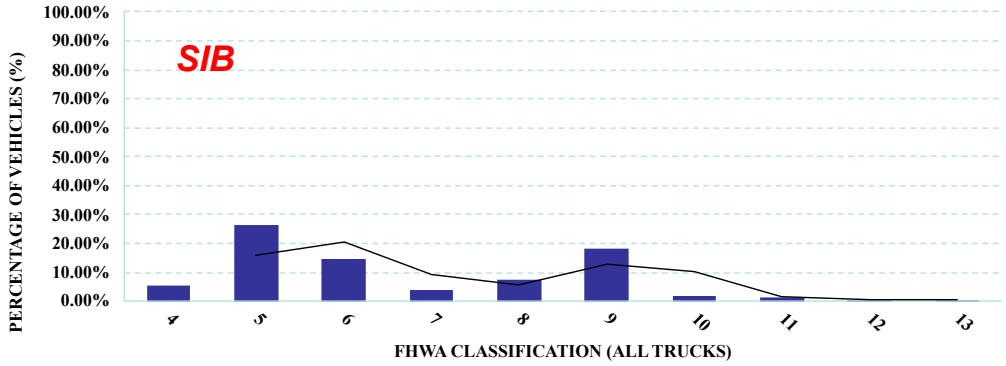

(b)

Figure 49: Distribution of Vehicle Classifications for IRD Data; (a) QB and (b) SIB

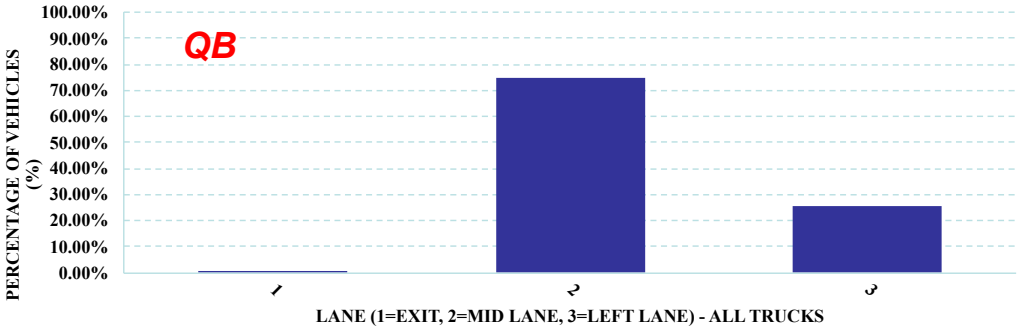

(a)

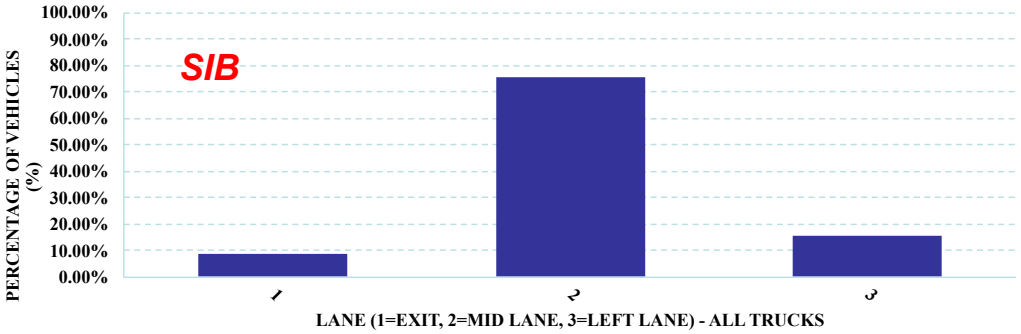

(b)

Figure 50: Distribution of Lanes of Vehicles for IRD Data; (a) QB and (b) SIB

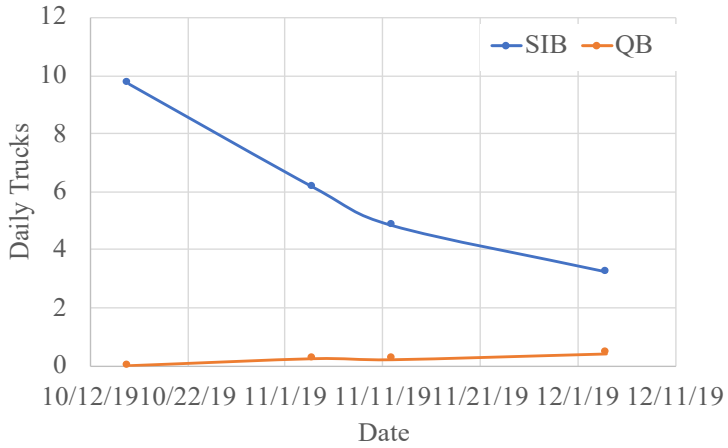

Figure 51: Number of Trucks above 150 Kips per Day

4.3 Accuracy Comparison of Quartz and PVDF Sensors

As discussed earlier, Class 9 trucks have been used to check the WIM data quality. Similarly, the team collected WIM records of Class 9 trucks collected from PVDF sensors and Quartz sensors, and compared them to validate the Quartz sensor accuracy. Two weeks of WIM data were compiled, and all the Class 9 records were selected from both Quartz and PVDF WIM datasets.

Figure 52 shows the GVW data obtained from Quartz sensors plotted against PVDF sensors per GVW range. At lower GVW ranges < 60 kips, the PVDF sensors overestimated the GVW by up to 78%. At higher GVW ranges > 80 kips, the PVDF sensors underestimated the GVW by 8%. At the GVW ranges between 60 kips and 80 kips, the PVDF sensors slightly overestimated the GVW by 14%. Figure 52(d) shows the combined results – yellow marks denote the Quartz GVW < 60 kips, blue marks denote the Quartz GVW 60-80 kips, and red marks indicate the Quartz GVW > 80 kips. One extreme case shows that when the Quartz sensors estimated 50 kips of GVW (legal weight), the PVDF sensors estimated > 100 kips (overweight).

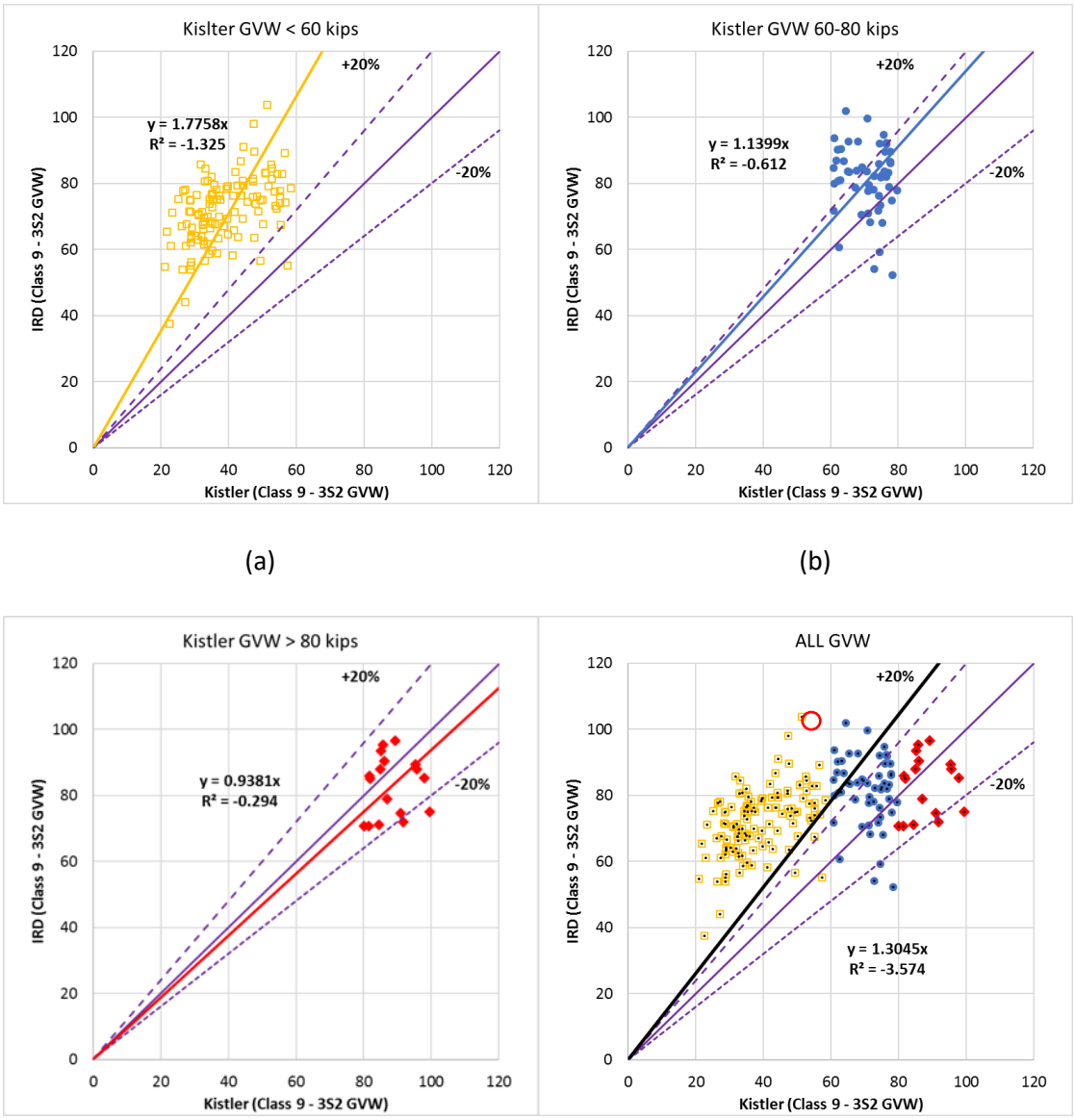

Figure 52: GVW Comparison between Quartz Sensors and PVDF Sensors per GVW Range; (a) GVW < 60 kips, (b) GVW 60-80 kips, (c) GVW > 80 kips, and (d) all GVWs

5. Conclusions and Recommendations

This study presented the effort to evaluate the damage induced by the overweight (OW) trucks in New York City and to implement the advanced weigh-in-motion (WIM) system for future autonomous OW enforcement practice to one testbed.

First, the bridge and pavement data were aggregated from the NBI database and bridge inspection reports of the NYC bridges and carefully reviewed and analyzed. Accordingly, the team established deterioration models for different types of structures to estimate their socio-economic impact on major highways. The study found that it would be of prime importance to aggregate the bridge inspection and pavement maintenance data from the agency's database for the development of the deterioration models. This would help identify the deterioration modes of different structure types, validate the deterioration models of different structure elements, and accurate life-cycle cost of infrastructure used in the analysis. This study also recommends collecting the bridge element construction and maintenance costs through analyzing the bidding contracts in the Bid Express bidding service (BIDX system). This is essential to perform a valid and reliable life cycle cost analysis including labor and material costs and to quantify the socio-economic impact.

Then, the team worked with NYCDOT to plan and establish a testbed along the triple cantilever of the Brooklyn-Queens Expressway (BQE) corridor to install, collect, and interpret various types of WIM sensors to effectively use the truck weight spectra. Two testbeds at the north and south portions of the triple cantilever section were considered based on various criteria and constraints to provide more reliable and accurate WIM data. Detailed field surveys, roughness measurement, and recommendations were discussed to select the most appropriate segments for implementation. The team installed two types of WIM sensors (PVDF and Quartz), and conducted a calibration test to determine the calibration factors and to test the accuracy of the implemented system. It was found that the Quartz sensors provide more reliable and accurate data compared to traditional piezo-type sensors (PVDF). In the end, the quality of WIM data was evaluated based on various quality control and quality assurance (QC/QA) methods. Moreover, the WIM data were analyzed to assess the live loads on the BQE. It was found that more than 10% of total trucks were identified as overweight trucks, and the maximum GVW was found to be more than 200 kips which imposed a significant impact on the NYC highway infrastructure. This confirms that autonomous OW enforcement would be imperative and vital to reducing the extent of the OW trucks.

References

1. ASTM E-1318-09, Standard Specification for Highway Weigh-In-Motion (WIM) Systems with User Requirements and Test Methods. ASTM International, PA, USA, 2017

2. Bushman, R. and A.J. Pratt. Weigh in Motion Technology - Economics and Performance. National Travel Monitoring Exposition and Conference, Charlotte, NC, 1998.

3. Dahlin, C. Proposed Method for Calibrating Weigh-In-Motion (WIM) Systems and for Monitoring That Calibration over Time. Transportation Research Record: Transportation Research Board, 1364, pp. 161–167, 1992

4. Mimbela, L.E.Y. and L.A. Klein. A Summary of Vehicle Detection and Surveillance Technologies used in Intelligent Transportation Systems. FHWA Report, FHWA Intelligent Transportation Systems Joint Program Office, 2000.

5. Monsere, C. and A.P. Nichols. Building a WIM Data Archive for Improved Modeling, Design, and Rating. North American Travel Monitoring Exhibition and Conference (NATMEC) 2008, Washington D.C. 2008

6. Nassif, H., K. Ozbay, H. Wang, R. Noland, P. Lou, S. Demiroluk, D. Su, C.K. Na, J. Zhao, and M. Beltran. Impact of freight on highway infrastructure in New Jersey. Final Report FHWA-2016-004, NJ Department of Transportation, 2015

7. Nassif, H., K. Ozbay, C.K. Na, P. Lou, G. Fiorillo, C.H. Park, and S. Demiroluk. Monitoring and Control of Overweight Trucks for Smart Mobility and Safety of Freight Operation, C2SMART Tier 1 University Transportation Center, Year 1 Final Report, 2018

8. Nichols, A. P., and D. M. Bullock. Quality control procedures for weigh-in-motion data, 2004

9. Ott, W.C. and A.T. Papagiannakis. Weigh-in-Motion Data Quality Assurance based on 3S2 Steering Axle Load Analysis. Transportation Research Record: Transportation Research Board, 1536, pp. 12–18, 1996

10. Southgate, H. F. Quality assurance of weigh-in-motion data. Washington, D.C: Federal Highway Administration, 2001

11. Transportation Research Board, Truck Size and Weight Limits Research Plan Committee. Research to Support Evaluation of Truck Size and Weight Regulations. Transportation Research Board Special Report 328, Transportation Research Board

12. Turner, S. Quality Control Procedures for Archived Operations Traffic Data: Synthesis of Practice and Recommendations. FHWA Final Report Texas Transportation Institute, 2007

13. Wei, T. and J.D. Fricker. Weigh-In-Motion Data Checking and Imputation, FHWA/IN/JTRP-2003/16, 2003

14. Zhang, L. An Evaluation of the Technical and Economic Performance of Weigh-In-Motion Sensing Technology. The Univ. of Waterloo, Thesis, 2007.